



## Paleogeography of the Congo/São Francisco craton at 1.5 Ga: Expanding the core of Nuna supercontinent

J.M. Salminen <sup>a,b,c,\*</sup>, D.A.D. Evans <sup>c</sup>, R.I.F. Trindade <sup>d</sup>, E.P. Oliveira <sup>e</sup>, E.J. Piispa <sup>f</sup>, A.V. Smirnov <sup>f</sup>

<sup>a</sup> Department of Physics, University of Helsinki, P.O. Box 64, Helsinki 00014, Finland

<sup>b</sup> Department of Geosciences and Geography, University of Helsinki, P.O. Box 64, Helsinki 00014, Finland

<sup>c</sup> Department of Geology & Geophysics, Yale University, New Haven, CT 06520-8109, USA

<sup>d</sup> Instituto de Astronomia, Geofísica e Ciências Atmosféricas, Universidade de São Paulo, Rua do Matão, 1226, São Paulo, SP 055080-090, Brazil

<sup>e</sup> Department of Geology and Natural Resources, Institute of Geosciences, University of Campinas-UNICAMP, P.O. Box 6152, Campinas 13083-970, Brazil

<sup>f</sup> Department of Geological and Mining Engineering and Sciences, Michigan Technological University, USA



### ARTICLE INFO

#### Article history:

Received 22 January 2016

Revised 8 August 2016

Accepted 11 September 2016

Available online 19 September 2016

#### Keywords:

Paleomagnetism

Supercontinent

Nuna

Columbia

Mesoproterozoic

Congo/São Francisco

### ABSTRACT

The Congo/São Francisco (C/SF) craton, one of the largest cratons in Proterozoic paleogeography, has been lacking reliable paleomagnetic data for the supercontinent Nuna interval (ca. 1600–1300 Ma). Here we provide a new paleomagnetic key pole for this craton from recently dated mafic dykes in the Curaçá ( $1506.7 \pm 6.9$  Ma) region of Brazil. The characteristic remanent magnetization (ChRM) direction  $D = 070.6^\circ$ ,  $I = 54.0^\circ$  ( $k = 22.1$  and  $a_{95} = 13.1^\circ$ ) corresponds with a paleomagnetic pole at  $10.1^\circ\text{N}$ ,  $009.6^\circ\text{E}$  ( $K = 15.6$ ,  $A_{95} = 15.8^\circ$ ), which places C/SF craton in moderate paleolatitudes at the time of remanence acquisition. Primary nature of the paleomagnetic remanence is supported by a baked-contact test. A similar ChRM direction was obtained for four Mesoproterozoic mafic intrusions in Chapada Diamantina region. The new pole, only from Curaçá, for C/SF allows us to reconstruct the extended core of the supercontinent Nuna at 1.5 Ga. Based on coeval 1.5 Ga and 1.38 Ga magmatism in Baltica, Siberia and C/SF, we favor the position where Southwest Congo is reconstructed against present South-Southeast (S-SE) Baltica. We explore two alternative 1.5 Ga reconstructions of Nuna's core. In both of them Baltica and Laurentia are shown in the well-defined NENA (Northern Europe North America) fit, together with Siberia in a tight fit to northern Laurentia. In reconstruction option A, more traditional fit of Amazonia with Baltica is shown, modified from the geologically based SAMBA (South AMerica BAltica) model to accommodate paleomagnetic data. In this option, however, West Africa must be extricated from SAMBA because C/SF has taken its place. For reconstruction option B, Amazonia is shifted to lie adjacent to NE Laurentia and West Baltica. In both options SW Congo is reconstructed against S-SE Baltica, but in option B there is a tighter fit between them, and there is a better match with our new paleomagnetic data for C/SF. In either option, separation of C/SF from Baltica and Siberia probably occurred at 1.38 Ga, the age of pronounced mafic magmatism throughout this sector of Nuna.

© 2016 Elsevier B.V. All rights reserved.

### 1. Introduction

The existence of the Paleoproterozoic supercontinent Nuna (a.k.a. Columbia, Hudsonland) has been proposed by many researchers (e.g., Williams et al., 1991; Hoffman, 1997; Meert, 2002; Rogers and Santosh, 2002; Zhao et al., 2004; Pesonen et al., 2003; Condie, 2004; Pisarevsky et al., 2014; Pehrsson et al., 2016). One of the main

geological arguments used for the existence of Nuna is the presence of 2.1–1.8 Ga orogens in the majority of continents (e.g., Zhao et al., 2004), and it was suggested that some or all of these orogens resulted from the assembly of this supercontinent. Paleomagnetism is the only quantitative method to generate Precambrian paleogeographic reconstructions, and recent paleomagnetic data have appeared to support, within the analytical uncertainties, a single NENA juxtaposition (Northern Europe – North America; Gower et al., 1990) between Baltica and Laurentia at ca. 1750–1270 Ma (Buchan et al., 2000; Salminen and Pesonen, 2007; Evans and Pisarevsky, 2008; Lubnina et al., 2010; Pisarevsky and Bylund, 2010; Salminen et al., 2014), forming a core element of Nuna. Adding cratons around this core has been a major initiative among

\* Corresponding author at: Department of Physics, University of Helsinki, P.O. Box 64, Helsinki 00014, Finland.

E-mail addresses: [johanna.m.salminen@helsinki.fi](mailto:johanna.m.salminen@helsinki.fi) (J.M. Salminen), [david.evans@yale.edu](mailto:david.evans@yale.edu) (D.A.D. Evans), [riftrindad@gmail.com](mailto:riftrindad@gmail.com) (R.I.F. Trindade), [elson@ige.unicamp.br](mailto:elson@ige.unicamp.br) (E.P. Oliveira), [ejpiispa@mtu.edu](mailto:ejpiispa@mtu.edu) (E.J. Piispa), [asmirnov@mtu.edu](mailto:asmirnov@mtu.edu) (A.V. Smirnov).

paleogeographers in recent years (e.g., Siberia, Evans and Mitchell, 2011; Evans et al., 2016a; North China, Zhang et al., 2012; Xu et al., 2014; India, Pisarevsky et al., 2013). The combined Congo/São Francisco (C/SF) craton has been placed adjacent to Baltica and Siberia based mainly on ages of mafic magmatism in the interval 1.5–1.38 Ga (Ernst et al., 2013), but paleomagnetic support for such a reconstruction was limited to an old result (Piper, 1974) that requires confirmation by more modern methods and field tests on the age of remanence acquisition.

Application of paleomagnetic data to the reconstructions requires not only a high reliability of the remanence directions, but also confidence in accurate dating of the rocks and their magnetic acquisitions. A reliable paleomagnetic pole generally fulfills at least three of the seven quality criteria of Van der Voo (1990). If two of these include adequately precise geochronological age and a positive paleomagnetic field test, the obtained paleomagnetic pole can be called a “key” pole (Buchan et al., 2000; Buchan, 2013). Paleomagnetic data from different continents allow comparison of lengths and shapes of apparent polar wander paths (APWPs) to test proposed long-lived proximities of the cratons. As long as these landmasses have traveled together they should have identical APWPs. In the absence of well-defined APWPs, pairs of coeval paleomagnetic poles from these cratons can be used for a rough test (e.g. Buchan et al., 2000; Evans and Pisarevsky, 2008). If the arc distance between two paleopoles with ages X and Y from one continent is the same as the arc distance between two paleopoles of the same ages from a second continent, then one can propose that those two continents traveled together (e.g. Evans and Pisarevsky, 2008; Pisarevsky et al., 2014). Moreover, these pairs of paleopoles should plot on top of each other within their error

limits, after Euler rotation to the continents' correct relative configuration. Unfortunately, many cratons –such as C/SF, Kalahari, and West Africa – have been entirely lacking good-quality paleomagnetic data for the Nuna interval.

A complementary approach to suggest neighborhood of cratons in the geological past is to compare coeval large igneous province (LIP) events for each craton (e.g. Bleeker and Ernst, 2006; Ernst and Bleeker, 2010). Specifically, cratons that share a number of coeval LIP events can be argued to have been “nearest neighbors”, whereas the lack of such matches suggests they were far away from each other during a given time period. Silveira et al. (2013) provided new U-Pb baddeleyite ages for the Chapada Diamantina and the Curaçá dykes in the SF craton ( $1501 \pm 9$  and  $1506.7 \pm 6.9$  Ma, respectively), and the recent U-Pb baddeleyite age of  $1502 \pm 5$  Ma (Ernst et al., 2013) for the Humpata sill in the Congo craton added a new Mesoproterozoic igneous event for C/SF craton. Another Mesoproterozoic igneous event of contemporaneous age for the combined C/SF craton is represented by the 1380 Ma Kunene Intrusive Complex in SW Angola (Dröppel et al., 2007; Ernst et al., 2008) and a nearly coeval mafic-ultramafic belt in the eastern portion of the Congo craton (Maier et al., 2007; Tack et al., 2010; Mäkitie et al., 2014), but is thus far not recognized in São Francisco. A Neoproterozoic igneous activity for the C/SF Craton is present on both blocks, the ca. 920 Ma Salvador dykes in the São Francisco Craton (Heaman, 1991; Evans et al., 2016b) and the contemporaneous Gangila/Mayumbian succession in the Congo craton (Tack et al., 2001). The 130 Ma basalts and sills from Paraná Basin of SF craton together with their counterpart in the southwest African territory, i.e. the Etendeka magmatic province, are a continental flood-basalt type LIP (Deckart et al., 1998;

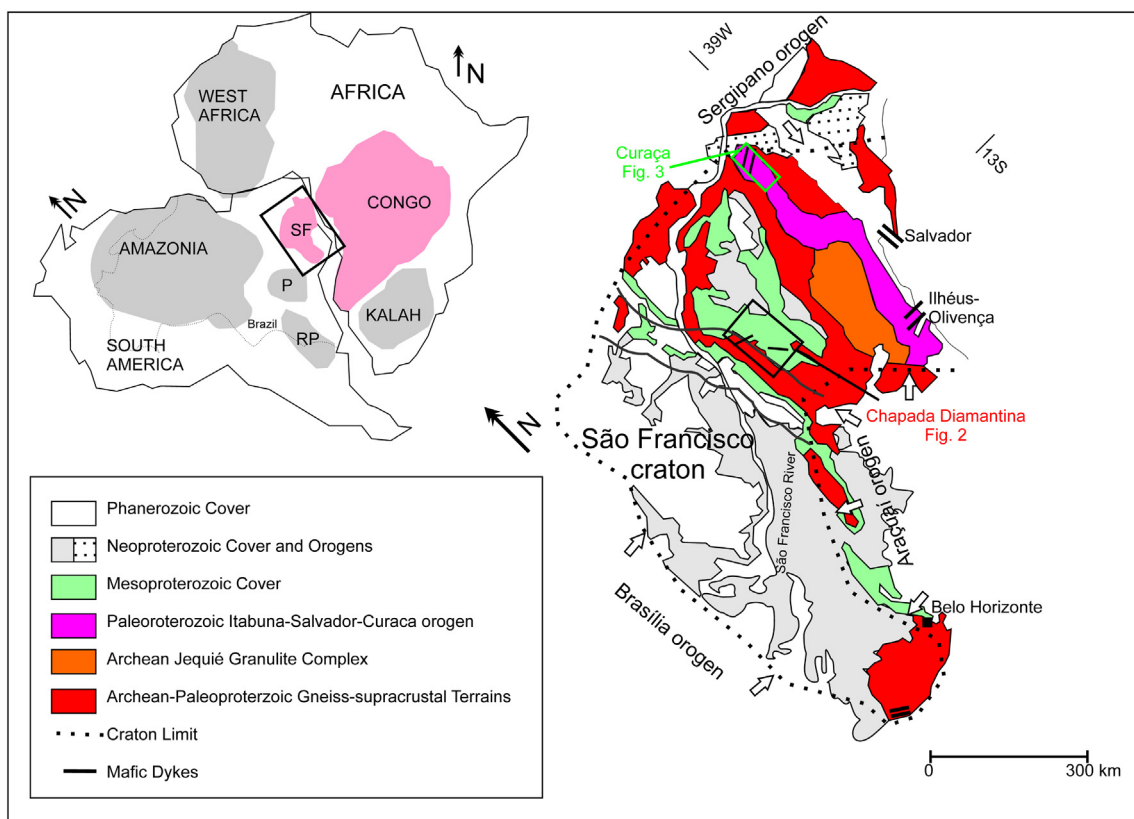


**Fig. 1.** Regional tectonic map of the Congo(C)/São Francisco(SF) craton after reconstruction of the South Atlantic Ocean (modified from Alkmim et al. (2006)). Cratons of western Gondwana-Land: Kalahari, P – Paranapanema, RP – Rio de la Plata, SF – São Francisco. Inset, Simplified geological map of the São Francisco Craton (modified after Silveira et al., 2013). Sampling areas of Curaçá (green) and Chapada Diamantina (black) are indicated with rectangles. White arrows signify vergence in bounding orogens. (For interpretation of the references to colour in this figure legend, the reader is referred to the web version of this article.)

Janasi et al., 2011). Their origin is related to the onset of break-up of South American and African continents.

The combined C/SF craton is one of the largest cratons in Meso-Neoproterozoic paleogeography. It is surrounded by latest Proterozoic to Cambrian orogens that welded together the supercontinent Gondwana (Fig. 1). Prior to that orogenic activity, a substantial proportion of the craton's margins were passive (Trompette, 1994). The margins were established in three separate rifting events: at ca. 920 Ma (Aracuaí and West Congolese; Tack et al., 2001), ca. 750 Ma (northern Damara and Lufilian; Hoffman and Halverson, 2008; Key et al., 2001), and a poorly dated but likely mid-Neoproterozoic event (Oubangui; Poidevin, 2007). The early- to mid-Neoproterozoic rifting events, along with at least one late Mesoproterozoic bounding orogen (Irumide belt; de Waele et al., 2009) and the presence of Neoproterozoic mobile belts (Araçuaí, Brasília, Riacho do Pontal, Rio Preto, and Sergipano) that surround SF, suggest that C/SF may have been a component of Rodinia supercontinent (Evans et al., 2016b), contrary to earlier suggestions

(Kröner and Cordani, 2003). Only a small number of paleomagnetic data exist for this large craton, and only few of those poles are of good quality. The motivation for the present study was to obtain high-quality paleomagnetic data from recently dated ( $1501 \pm 9.1$  Ma;  $1506.7 \pm 6.9$  Ma U-Pb; Silveira et al., 2013) early Mesoproterozoic dyke swarms in the Chapada Diamantina and Curaçá regions in São Francisco craton (Figs. 2 and 3) and to examine the C/SF craton's possible placement within Nuna.

## 2. Geology

The terranes of São Francisco craton aggregated during the time interval 2.1–1.8 Ga (Teixeira and Figueiredo, 1991). Many other continents also contain 2.1–1.8 Ga orogens (e.g., Zhao et al., 2004), which are interpreted to result from the initial assembly of supercontinent Nuna (Hoffman, 1997). The major basement rocks of the SF craton are Archean to Paleoproterozoic high-grade

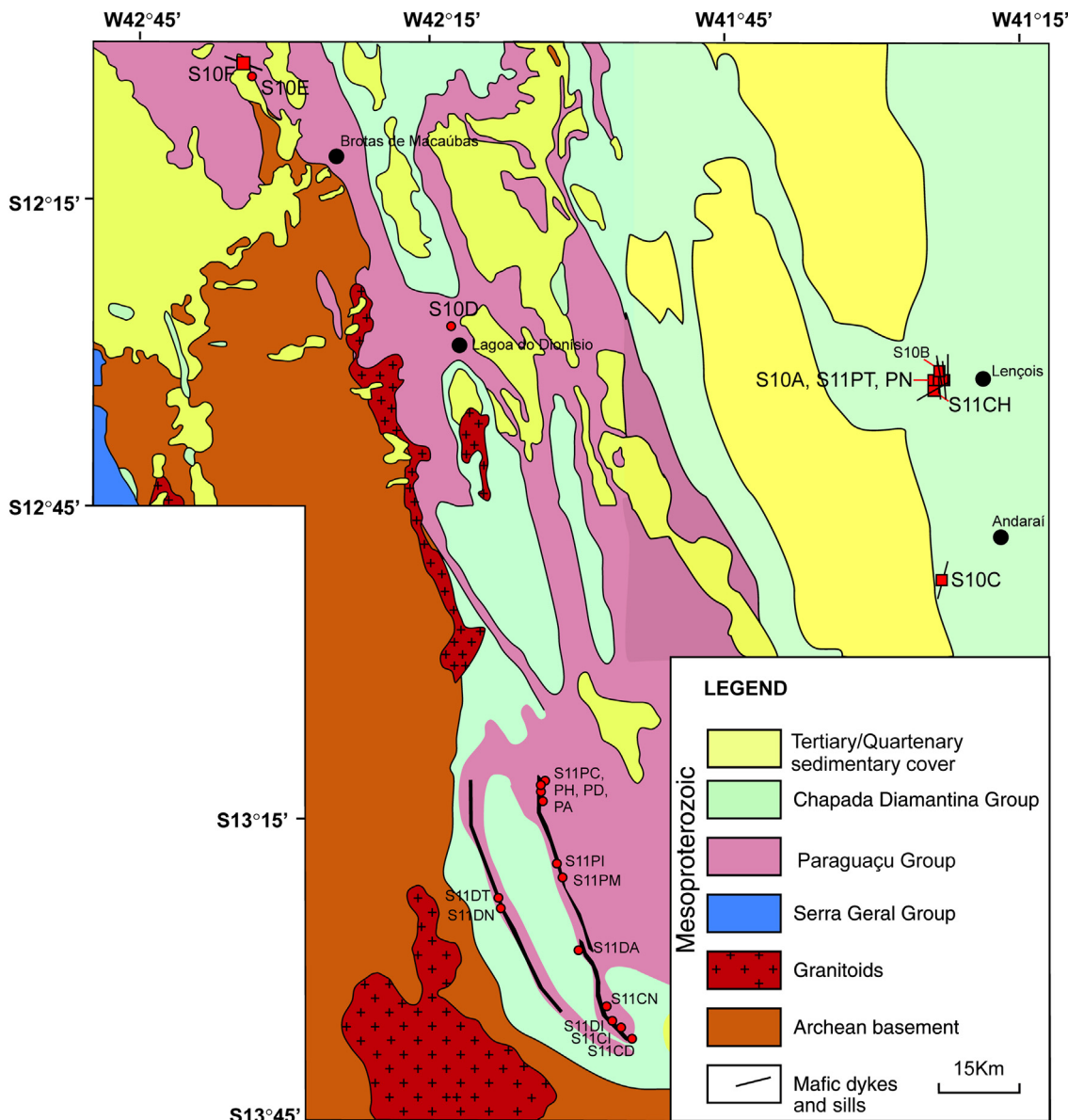


**Fig. 2.** Sampling sites in Chapada Diamantina. Modified after Silveira et al. (2013) and Batillani et al. (2007). Squares indicate sites that gave consistent paleomagnetic results. Orientation of the dyke is indicated with the black lines.

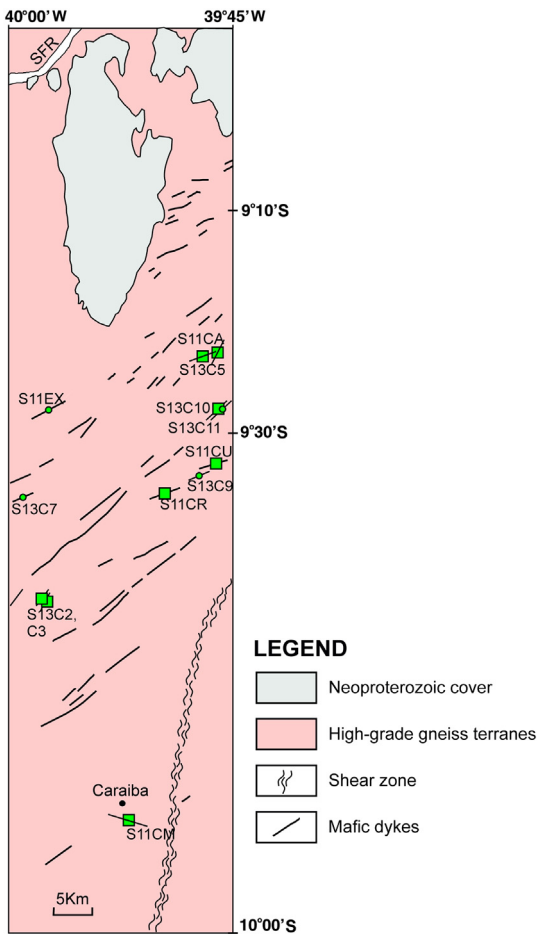


**Fig. 3.** Sampling sites in Curaçá region. Modified after Silveira et al. (2013). Squares indicate sites that showed consistent paleomagnetic results. SFR = São Francisco River.

migmatite and granulite gneisses, and granite-greenstone associations (Barbosa et al., 2003; Barbosa and Sabaté, 2004; Teixeira et al., 2000). Meso- to Neoproterozoic sedimentary rocks of the Espinhaço Supergroup and the São Francisco Supergroup (Alkmim et al., 1993; Barbosa et al., 2003; Danderfer et al., 2009) overlie these rocks.

Espinhaço Supergroup is exposed at the Chapada Diamantina area, where it is divided into three main stratigraphic units, the Rio dos Remédios, Paraguaçu, and Chapada Diamantina Groups (Pedreira, 1994; Guimarães et al., 2005b; Pedreira and De Waele, 2008). A magmatic U-Pb zircon age of  $1748 \pm 1$  Ma (Babinski et al., 1994) for the Rio dos Remédios is interpreted to represent the beginning of the Espinhaço Supergroup sedimentation. Paraguaçu Group includes the shallow-water marine, deltaic, fluvial and eolian deposits of the Mangabeira and Açuá Formations (Pedreira, 1994; Guimarães et al., 2005; Pedreira and De Waele, 2008). Guadagnin and Chemale (2015) provided  $^{207}\text{Pb}/^{206}\text{Pb}$  (zircon) data for the Mangabeira formation, where the main zircon age peak was determined from 112 grains (65%) with a weighted mean age of  $2080 \pm 8$  Ma and the three youngest zircon grains yielded and U-Pb age of  $1739 \pm 40$  Ma. The top most unit of the Espinhaço Supergroup, Chapada Diamantina Group, is divided to continental deposits of Tombador Formation, the transgressive shallow marine fine-grained package of the Caboclo Formation, and fluvial strata of the Morro do Chapéu Formation (Guadagnin et al., 2015 and references therein). Recently Guadagnin et al. (2015) suggested a depositional age for the top of the Tombador Formation by dating a  $1436 \pm 26$  Ma ( $^{207}\text{Pb}/^{206}\text{Pb}$ , zircons)

crystal-rich volcaniclastic unit at the Ribeirão de Baixo section near Lençóis. For Caboclo Formation, Babinski et al. (1993) provided a whole-rock Pb-Pb isochron depositional age of ca. 1.2 Ga.

The recently dated, fresh, undeformed, and unmetamorphosed  $1501.0 \pm 9.1$  Ma (U-Pb, baddeleyite; Silveira et al., 2013) dolerite dyke of Chapada Diamantina (Fig. 2) intruded the Mangabeira Formation (Paraguaçu Group). Coeval 1.5 Ga magmatism in the Chapada Diamantina region is suggested to be rather widespread. Babinski et al. (1999) provided an age of  $1514 \pm 22$  Ma (U-Pb, zircon) for gabbro sill intruding the Mangabeira Formation in Lagoa de Dentro in the Brotas de Macaúbas region. Battilani et al. (2005, 2007) dated  $1512 \pm 6$  Ma and  $1514 \pm 5$  Ma (Ar-Ar, muscovites) muscovite-martite (iron-oxide) dykes near Lençóis cutting the Tombador Formation. These results challenge the recent suggestion of Guadagnin et al. (2015) for the age estimate of 1.42–1.43 Ga for the upper part of Tombador Formation. Moreover, Guimarães et al. (2005a) dated a  $1496.1 \pm 3.2$  Ma (U-Pb, zircon) mafic dyke in the Lagoa do Dionísio area, which intruded the Morro do Chapéu Formation, challenging the prosed depositional age of 1.2 Ga for the underlying Caboclo Formation (Babinski et al., 1993). These conflicting ages demand further stratigraphic work in the Chapada Diamantina region.

In the northeast corner of the SF craton, the  $1506.7 \pm 6.9$  Ma (U-Pb, baddeleyite Silveira et al., 2013) Curaçá dolerite dyke swarm (Fig. 3) intrudes Archean to Paleoproterozoic metamorphic rocks of the Caraíba complex, and is unconformably overlain by Neoproterozoic rocks of the Canudos Group (Bastos Leal et al., 1995; Oliveira and Tarney, 1995). The dykes are vertical and trend typically NE-SW. Dyke width varies from a few centimeters to several tens of meters. Bastos Leal (1992) reported Rb-Sr ages in the range of 700–650 Ma for the intrusion of the Curaçá dyke swarm. These results indicated a possible connection to the Brasiliano/Pan-African cycle by recording the possible regional metamorphism.

### 3. Sampling and methods

#### 3.1. Sampling

Standard 2.5-cm diameter cores were collected with a portable field drill from 11 different mafic cooling units (dykes and sills) in Chapada Diamantina (Fig. 2; Table 1). Cored samples were oriented using solar and/or magnetic compasses. At many of the sites intrusions were outcropping only as boulders (circles in Fig. 2). Number of samples taken from each unit is shown in Table 1. Results show that only five dykes (S10B, S10C, S11CH, S11PN, S11PT: squares in Fig. 2) and two sills (S10A, S10F: squares in Fig. 2) intruding the Chapada Diamantina Group were *in situ*. Site S10F intrudes the Mangabeira Formation (Paraguaçu Group). The geochronology site of Guimarães et al. (2005a) in the Lagoa do Dionísio area (U-Pb zircon age of  $1496.1 \pm 3.2$  Ma; S10D in Fig. 2) intruding the Morro do Chapéu is included to sampled sites. There we sampled five different outcrops (three samples from each). It turned out that the intrusion was outcropping only as boulders, which we discovered (based on the paleomagnetic remanence data) to be individually rotated within the soil and thus not useful for pole calculation. We sampled three mafic sills intruding Paraguaçu group at the southern part of Chapada Diamantina. These sills were suggested to be coeval with the one in Lagoa do Dionísio ( $1496.1 \pm 3.2$  Ma; Guimarães et al., 2005a), but they were outcropping only as boulders. Baked-contact test (Everitt and Clegg, 1962) was attempted at site S10C, which was the only site in Chapada Diamantina where also the host rock was exposed. In addition to these dykes and sills in Chapada Diamantina, we attempted for conglomerate test by sampling mafic clasts intruding the Mangabeira Formation (Paraguaçu group). Samples were taken from a large, coherent but

**Table 1**

Paleomagnetic data of this study for mafic intrusions in Curaçá and Chapada Diamantina regions in Brazil.

Site	Str/dip	Width (m)	Age (Ma)	Lat (°N)/Long (°E)	(N)/b/n	D (°)	I (°)	$\alpha 95$ (°)	k	Plat (°N)	Plong (°E)	A95 (°)	K
<b>Accepted to the mean</b>													
<b>Curaçá</b>													
S11CA: dyke	27/90	15		−9.40/320.17	11/9	091.3	50.4	4.8	115.0	−05.9	020.5		
S11CM: dyke	107/77	0.4		−9.88/320.14	13/11	063.0	39.9	6.9	44.6	19.7	020.9		
S13C2: dyke	37/70	2		−9.69/319.97	8/7	069.5	38.8	9.5	41.7	15.2	023.7		
S13C3: dyke	27/70	0.4		−9.69/319.97	8/8	080.4	40.3	12.1	19.0	04.7	025.2		
S13C5: dyke	67/?	0.05		−9.39/320.16	11/6	032.6	77.1	12.2	31.3	11.4	333.4		
S13C10: dyke	47/80	1		−9.48/320.21	7/6	055.3	63.3	20.7	11.4	14.6	355.4		
S11CU: baked host				1506.7 ± 6.9 <sup>a</sup>	−9.57/320.21	3/3	073.0	62.5	21.1	35.0	05.3	002.4	
Mean Curaçá						7°/62/51	070.6	54.0	13.1	22.1	10.1	009.6	15.8 15.6
Host rock supporting primary magnetization													
S11CA: baked host				−9.40/320.17	3/1	112.2	67.1			−21.4	000.1		
S11CA: unbaked host				−9.40/320.17	1/1	192.1	66.0			−49.8	307.7		
<b>Excluded</b>													
<b>Chapada Diamantina <i>in-situ</i></b>													
S10A: sill		?		−12.57/318.59	10/9	056.1	60.8	11.9	19.7	16.9	358.4		
S11CH: dyke	60/?	7		−12.59/318.61	7/7	048.2	57.2	5.5	123.0	23.0	357.1		
S11PN: dyke	335/?	5		−12.57/318.60	6/6	079.8	70.1	4.9	189.5	−04.3	353.6		
S11PT: dyke	335/?	>20		−12.57/318.59	6/4	109.2	63.1	14.2	42.6	−21.7	005.0		
Mean Chapada Diamantina (CD)					4°/29/26	070.9	64.9	15.6	35.8	02.8	358.9	24.1	15.5
MEAN Curaçá + CD					11°/77	070.7	58.0	9.3	25.0	07.5	005.7	11.9	15.6
S10B: dyke	327/90	?		−12.56/318.60	11/11	352.6	−37.2	12.2	25.4	52.7	67.9		
S10C: dyke	92/90	1		−12.81/318.66	9/8	330.6	62.1	14.8	15.0	27.7	294.9		
S10C: baked host				−12.81/318.66	5/4	005.0	36.3	10.9	72.1	56.7	327.2		
<b>Chapada Diamantina not <i>in-situ</i></b>													
S10D: dyke, 5 blocks, not <i>in-situ</i>	−	−	1496 ± 3.2 <sup>b</sup>	−12.45/317.77	15/0								
S10E: conglomerate test				−12.02/317.39	12								
S10F: sill	x/?	?		−12.02/317.40	8/0	359.0	56.8	21.8	7.4	34.1	343.7		
S11CN: mafic sill 1, 7 blocks, not <i>in-situ</i>				−13.49/317.96	9/0								
S11CI: mafic sill 1, 10 blocks, not <i>in-situ</i>				−13.56/317.97	10/0								
S11CD: mafic sill 1, 10 blocks, not <i>in-situ</i>				−13.58/317.97	10/0								
S11DI: mafic sill 1, 3 blocks, not <i>in-situ</i>				−13.54/317.96	6/0								
S11DA: mafic sill 1, 4 blocks, not <i>in-situ</i>				−13.46/317.86	8/0								
S11DN: mafic sill 3, 2 blocks, not <i>in-situ</i>				−13.37/317.90	6/0								
S11DT: mafic sill 3, 2 blocks, not <i>in-situ</i>				−13.36/317.90	6/0								
S11PM: mafic sill 2, 1 blocks, not <i>in-situ</i>				−13.32/317.79	6/0								
S11PI: mafic sill 2, 3 block, not <i>in-situ</i>				−13.30/317.79	6/0								
S11PA: mafic sill 2, 3 blocks, not <i>in-situ</i>				−13.24/317.79	6/0								
S11PC: mafic sill 2, 2 blocks, not <i>in-situ</i>				−13.19/317.80	6/0								
S11PD: mafic sill 2, 3 blocks, not <i>in-situ</i>				−13.23/317.79	7/0								
S11PH: mafic sill 2, 3 blocks, not <i>in-situ</i>				−13.22/317.79	7/0								
<b>Curaçá not included to the mean</b>													
S11EX: dyke, 4 blocks, not <i>in-situ</i>	60/?	15		−9.48/320.04	15/0								
S11CR: dyke	70/90	9		−9.61/320.19	3/3	167.4	24.1	4.8	672.5	77.3	214.6		
S11CR: baked host				−9.61/320.19	2/1	145.8	23.2			56.3	222.4		

(continued on next page)

Table 1 (continued)

Site	Str/dip	Width (m)	Age (Ma)	Lat (°N)/Long (°E)	(N)/b/n	D (°)	I (°)	$\alpha 95$ (°)	k	Plat (°N)	Plong (°E)	A95 (°)	K
S13C07: dyke, 3 blocks, not in-situ	57/?	35		-9.61/319.89	9/0								
S13C09: dyke, 3 blocks, not in-situ	67/?	15		-9.60/320.20	9/0								
S13C11: dyke	47/?	15		-9.48/320.21	9/7	080.7	54.4	22.2	8.4	-0.9	-0.9	012.7	

<sup>a</sup> Age for the dyke from Silveira et al. (2013).<sup>b</sup> Age for the dyke from Guimaraes et al. (2005). Str/dip – strike and dip of the intrusion. lat/long – sampling latitude and longitude. (N)/b/n – number of (sites)/samples taken/samples showing the ChRM. D – declination. I – inclination.  $\alpha 95$  – the radius of the 95% confidence cone in Fisher (1953) statistics. k – Fisher (1953) precision parameter. Plat (Plong) – latitude (longitude) of the pole. A95 – radius of the 95% confidence cone. K – Fisher (1953) precision parameter of pole. Three different 1496.1 ± 3.2 Ma (U-Pb; zircon; Guimaraes et al., 2005) mafic sills were sampled: 1. (S11CD, S11CI, S11CN, S11DA, S11DI); 2. (S11PA, S11PC, S11PH, S11PI, S11PD, S11PM) and 3. (S11DN, S11DT).

out-of-place block that was excavated from a quarry along the road to Brotas de Macaúbas (site S10E). Because the sampled conglomerate is older than the 1.5 Ga mafic magmatism investigated in this study, it does not conform to the strict definition of the conglomerate test; nonetheless, the mafic igneous nature of sampled clasts and geographic proximity to one of the 1.5 Ga sample sites, provide insight into whether the area has been regionally remagnetized.

Altogether, 12 different mafic dykes were sampled from Curaçá region as either standard-size oriented cores or oriented block samples. Also in many of the Curaçá region dykes we suspected that the sampled parts of the dykes were not *in situ*, as the dykes composed only of separate boulders. Ultimately, eight *in situ* dyke sites (S11CA, S11CM, S11CU, S11CR, S13C2, S13C3, S13C5, and S13C10) were sampled (squares in Fig. 3). Baked-contact tests were attempted at four of these sites (S11CA, S11CM, S11CR, and S11CU). At the geochronology site S11CU (1506.7 ± 6.9 Ma; Silveira et al., 2013) the *in situ* dyke itself was very weathered and appeared fresher only in loose boulders. Five samples were taken from the weathered *in situ* part of the dyke S11CU and three samples were collected from each of three fresh-looking baked host rocks.

### 3.2. Laboratory methods

Paleomagnetic measurements of all the Chapada Diamantina and major part of Curaçá samples were conducted in the magnetically shielded room of the paleomagnetic laboratory of the Department of Geology and Geophysics at Yale University, USA. Samples from additional Curaçá sites were measured in the Solid Earth Geophysics Laboratory at the University of Helsinki, Finland. At Yale University, after the measurement of natural remanent magnetization (NRM), samples were placed into liquid nitrogen in a null field to demagnetize viscous remanent magnetization (Borradaile et al., 2004). The samples were then thermally demagnetized using a nitrogen-atmosphere ASC Scientific model TD-48SC furnace to separate the characteristic remanent magnetization (ChRM) component. A few sister specimens were demagnetized stepwise using the alternating field (AF) method with a Molspin tumbler apparatus with self-reversing spin mechanism at Yale University. In the Yale laboratory, remanent magnetization was measured using an automated sample-changing system attached to a 2G (now WSGI) cryogenic magnetometer (Kirschvink et al., 2008). At the University of Helsinki, several additional Curaçá samples were demagnetized using the in-line static 3-axis AF system paired to the 2G cryogenic magnetometer, and some were thermally demagnetized using an argon-atmosphere ASC Scientific model TD-48SC furnace. The thermal method was effective and provided stable results. The AF method produced spurious results for Chapada Diamantina samples, but it produced stable data for Curaçá samples. Vector components were isolated using principal component analysis (Kirschvink, 1980) and analyzed with Fisher (1953) statistics giving unit weight to each specimen to compute a site mean.

Magnetic mineralogy was investigated by several methods using powdered whole-rock samples. Temperature dependence of low-field magnetic susceptibility was measured from -192 °C to ~700 °C (in argon) followed by cooling back to room temperature at Yale University using AGICO KLY4-CS Kappabridge. Room-temperature hysteresis properties using a vibrating sample magnetometer (from Princeton Measurements Corporation) were measured to determine domain states of magnetic carriers in both at the Institute for Rock Magnetism (IRM) at University of Minnesota (USA) and in the University of Helsinki (Finland). Low-temperature remanence measurements to explore magnetic carriers were conducted at IRM using a Magnetic Properties Measurement System

(MPMS) superconducting quantum interference device (SQUID) magnetometer (from Quantum Design, Inc.).

## 4. Results

### 4.1. Rock magnetic results

#### 4.1.1. Thermomagnetic analyses

Examples of thermomagnetic analyses are shown in Fig. 4. High temperature heating curves show the presence of both magnetite and hematite in Chapada Diamantina samples with Curie temperature of 586–589 °C and Neél temperature of 646–690 °C, respectively. The Chapada Diamantina samples S11CH7, S11PN1, S10E9 show nearly reversible heating and cooling curves. Samples S10A and S19F10 show pronounced irreversible cooling curve indicating

the formation of a magnetite during the heating. Low-temperature Verwey transition (Verwey, 1939) is not obtained for measured dykes and sills from Chapada Diamantina. Exceptional are the mafic clasts from a conglomerate site (S10E), which show two low-temperature transitions, at -162 °C and at -152 °C indicating stoichiometric and non-stoichiometric magnetite. Samples from site S10B (sample S10B6 in Fig. 4) shows a distinct pronounced peak around the Neél temperature of hematite. This kind of behavior has previously been obtained for impure hematite (Petrovský and Kapička, 2006).

High-temperature heating curves show the presence of magnetite in Curaçá samples, with Curie temperatures 585–586 °C (Fig. 4). Samples from Curaçá show pronounced irreversible cooling curves indicating the formation of magnetite during the heating. Samples S11CA2 and S11CM4 show pronounced Hopkinson effects. Low-temperature measurements show the presence of

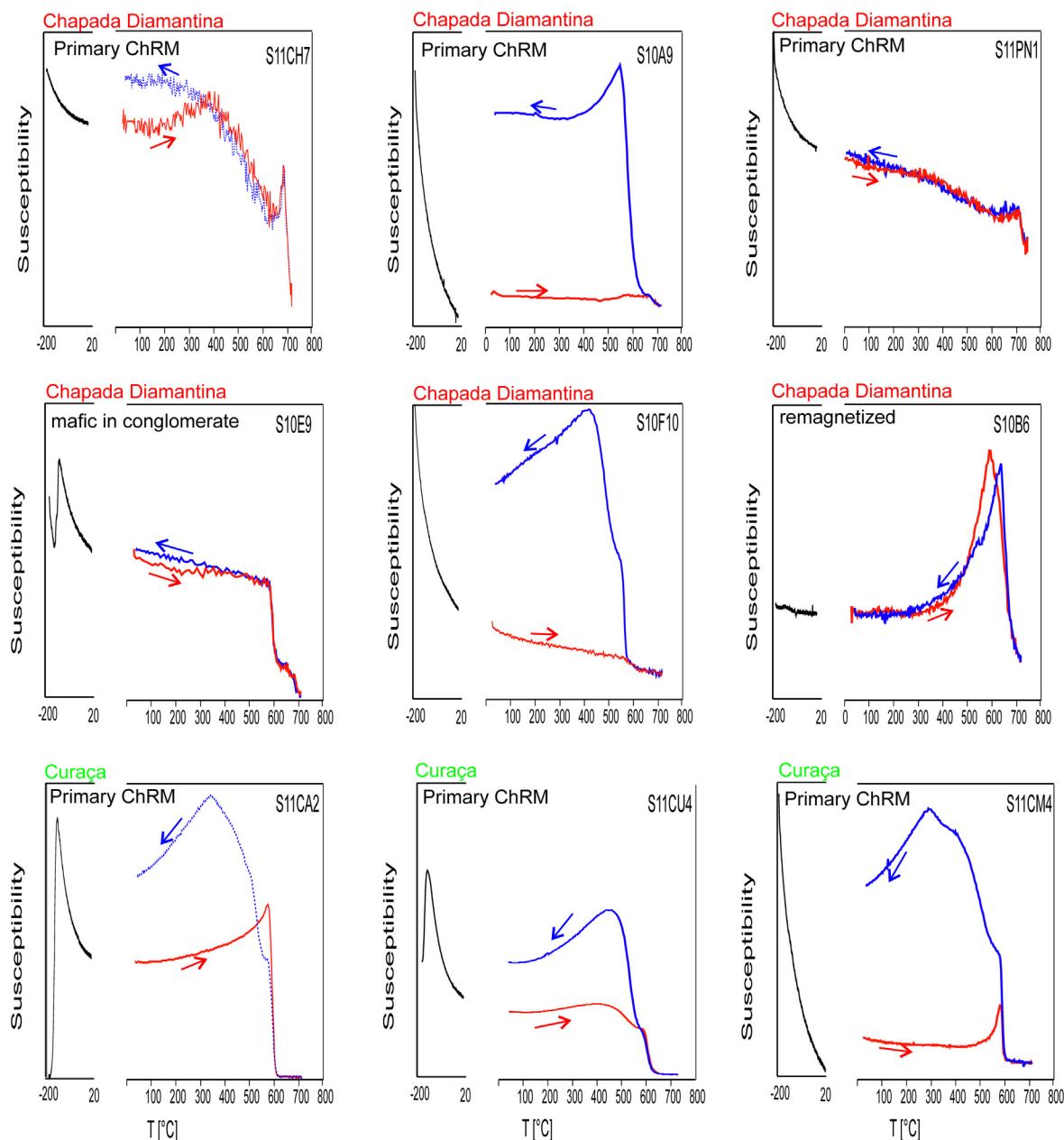


**Fig. 4.** Thermomagnetic curves for mafic dyke and sill samples for Chapada Diamantina and Curaçá samples. Low-field thermomagnetic curves measured from -192 °C to room temperature (in air) and from room temperature to 700 °C followed by cooling back to room temperature (in argon) (red solid line: heating, blue dotted line: cooling). Y-axis shows susceptibility in arbitrary units. (For interpretation of the references to colour in this figure legend, the reader is referred to the web version of this article.)

nearly stoichiometric magnetite (Verwey, 1939) for samples S11CA2 and S11CU4.

#### 4.1.2. Hysteresis properties

Examples of hysteresis results are shown in Fig. 5. Magnetic hysteresis loops for Chapada Diamantina samples show typical behavior of a high-coercivity mineral indicating the presence of hematite. Sample S10E9 is an exception, showing characteristics of magnetite. The hysteresis loops for Curaçá samples (Fig. 5, samples S11CA2 and S11CU4) are typical for a low-coercivity magnetic mineral phase indicating the presence of magnetite.

### 4.2. Paleomagnetism

#### 4.2.1. Primary magnetization

Paleomagnetic results are listed in Table 1, and representative demagnetization behaviors are illustrated in Figs. 6–8. The characteristic remanence (ChRM) direction, with easterly declinations and downward pointing intermediate to steep inclinations, is obtained from four sites (S10A, S11CH, S11PN, and S11PT) in Chapada Diamantina (Fig. 6) and from seven sites (S11CA, S11CM, S11CU, S13C2, S13C3, S13C5, and S13C10) in Curaçá (Fig. 7). Only site-means derived from three or more samples and with Fisher (1953) precision parameter ( $k$ ) higher than 11 are included in the overall mean calculations. Due to these criteria, site S13C11 that

shows a similar ChRM direction is excluded from the mean calculation. Sites S10B, S10C and S10F at Chapada Diamantina and site S11CR in Curaçá were *insitu*, but did not show similar characteristic remanence directions to other sites, as will be discussed below.

Due to hematite being the major carrier of the magnetization in the Chapada Diamantina samples, AF demagnetization was insufficient to remove the remanence, but instead the samples were amenable to thermal demagnetization. ChRMs with unblocking temperatures from 640 °C to 680 °C were obtained from four sites (S10A, S11CH, S11PN, and S11PT) (Fig. 6, Table 1).

Samples from Curaçá were stable to both thermal and AF demagnetization methods. ChRMs were obtained with unblocking temperatures up to 585 °C and in range of 30–160 mT (AF fields).

Six Curaçá dyke sites (S11CA, S11CM, S13C2, S13C3, S13C5, and S13C10) fulfill our selection criteria (three or more samples and Fisher (1953)  $k$ -value higher than 11), and we also include the baked host rock of the dated dyke site, even though the dyke itself did not give reasonable results.

**4.2.1.1. Baked contact test.** Baked-contact tests were performed at five sites (S10C, S11CA, S11CR, S11CM, and S11CU).

At Curaçá sites S11CA and S11CU, the baked rocks show the ENE steeply or intermediately downward ChRM direction, same as the intruding dykes. The baked contact test results at site S11CA are shown in Fig. 8. The baked host sample directly from the

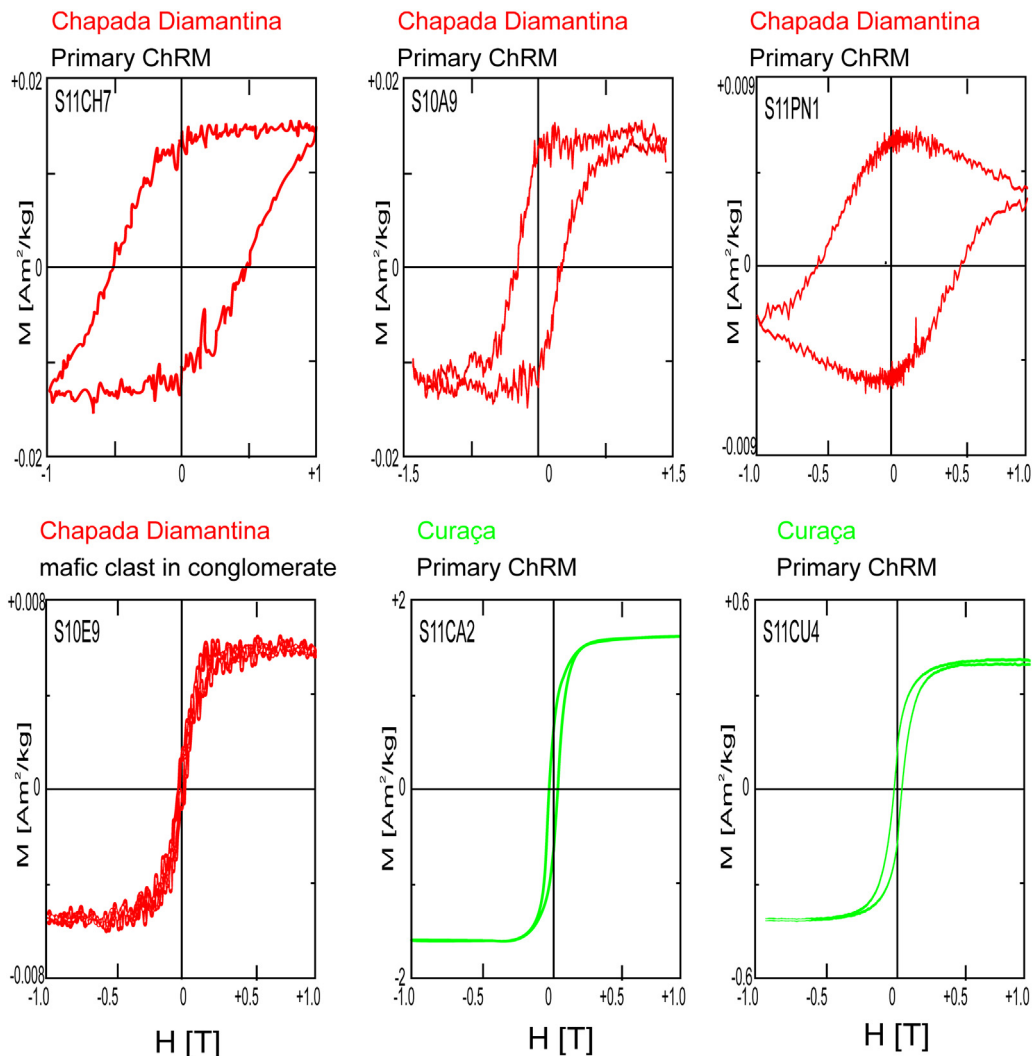
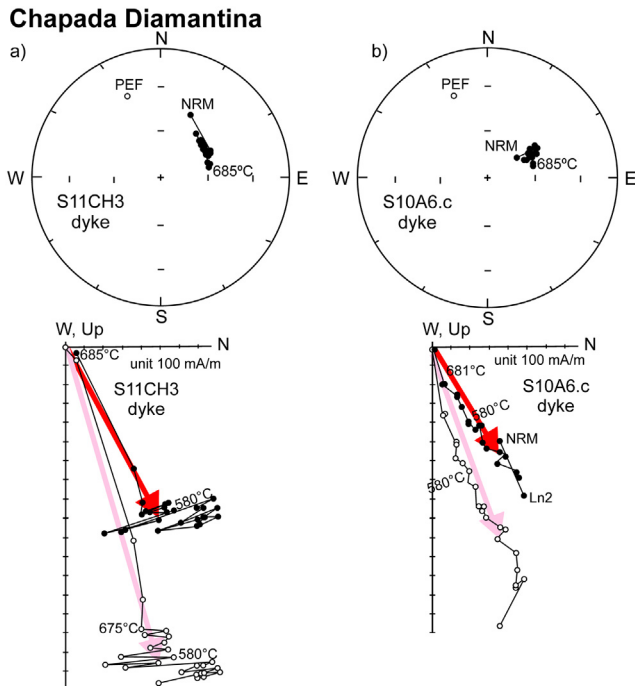


Fig. 5. Magnetic hysteresis loops after paramagnetic slope correction.



**Fig. 6.** Examples of Chapada Diamantina palaeomagnetic data. Representative demagnetization data for (a) dyke S11CH, and (b) dyke S10A. Red arrows indicate 1.5 Ga characteristic remanence direction. On stereoplots, solid symbols represent lower hemisphere vectors, and open symbols represent upper hemisphere vectors. On orthogonal projection diagrams, solid symbols show projections onto the horizontal plane (declination), and open symbols show projections onto the vertical plane (inclination). PEF – Present Earth's field direction at sampling sites. (For interpretation of the references to colour in this figure legend, the reader is referred to the web version of this article.)

S-contact of the dyke shows a similar ChRM to that of the dyke. The remanence direction of the illustrated unbaked host rock sample taken 100 m from the dyke starts (NRM-LN2-100 °C) from present Earth magnetic field direction and shows a southward and steeply to moderately downward pointing ChRM direction. This site provides a full positive baked contact test indicating that the obtained ENE ChRM has the primary nature and is not due to any later remagnetization. Baked samples were collected also from the geochronology site of Silveira et al. (2013) at Curaçá (1506.7 ± 6.9 Ma; S11CU), where the dyke itself was weathered *in situ* or fresher in loose boulders. The weathered part of the dyke was remagnetized and did not yield any meaningful paleomagnetic results. The baked host rock samples, however, give E steeply to moderately downward pointing ChRM direction (Fig. 7c) similar to that obtained from other *in situ* dykes in Curaçá and in Chapada Diamantina. The site S10C at Chapada Diamantina did not show the ENE ChRM and will be discussed in Section 4.2.2.

**4.2.1.2. Conglomerate test.** We sampled mafic clasts from a conglomerate of the 1.74–1.51 Ga Mangabeira formation (Babinski et al., 1999; Guimarães et al., 2005a; Silveira et al., 2013; Guadagnin and Chemale, 2015) in a quarry along the road to Brotas de Macaúbas for a conglomerate test (site S10E) as described above (Chapter 3.1). The remanence directions from different clasts are uniformly (“randomly”) distributed (Fig. 9) indicating the passage of the test. A single clast was large enough to be doubly cored, and directions from the two cores were similar, adding reliability to the test result. Chapada Diamantina sites showing ChRM are intruding Tombador Formation and have distinct magnetic mineralogy, so the test is not specifically relevant to the 1.5 Ga intrusions; however, it gives additional evidence for the absence of regional remagnetizing events on the Chapada Diamantina area.

**4.2.1.3. New paleopole for Congo/São Francisco craton.** Positive baked contact test proves that ENE steeply or intermediately downward ChRM direction obtained for Curaçá dykes has the primary origin. The mean for the seven accepted sites from Curaçá is  $D = 070.6^\circ$ ,  $I = 54.9^\circ$ ,  $k = 22.1$ ,  $a_{95} = 13.1^\circ$  (Fig. 10; Table 1). The corresponding mean of the seven site-mean VGPs is at  $10.1^\circ\text{N}$ ,  $009.6^\circ\text{E}$ ,  $K = 15.6$ ,  $A_{95} = 15.8^\circ$ . The mean of four dykes from Chapada Diamantina intruding the Tombador formation is  $D = 070.9^\circ$ ,  $I = 64.9^\circ$ ,  $k = 35.8$ ,  $a_{95} = 15.6^\circ$  (Fig. 10; Table 1). The corresponding mean Virtual Geomagnetic Pole (VGP), calculated as a mean of individual dyke VGPs, is  $02.8^\circ\text{N}$ ,  $358.9^\circ\text{E}$ ,  $K = 15.5$ ,  $A_{95} = 24.1^\circ$ . Positive conglomerate test on mafic clasts in the Mangabeira Formation indicates that there is no regional remagnetization event on the Chapada Diamantina area. The age constraint for the sampled Chapada Diamantina dykes showing ChRM is challenging since none of the dykes showing ChRM have been dated. They all intrude the Tombador Formation. Recently a depositional age of 1.43–1.42 Ga for the Tombador Formation was suggested by Guadagnin et al. (2015). Yet there are other evidence that  $1512 \pm 6$  Ma and  $1514 \pm 5$  Ma (Ar-Ar, muscovites) muscovite–magnetite (iron-oxide) dykes near Lençóis cut the Tombador Formation (Battilani et al., 2005, 2007). Moreover Guimarães et al. (2005a) dated a dyke intruding the Morro do Chapéu Formation above the Tombador Formation to be  $1496.1 \pm 3.2$  Ma (U-Pb, zircon). Due to these challenges for age constraints from Chapada Diamantina, in the further discussion for the paleogeographic reconstruction of the C/SF we will rely only on the results from the Curaçá dykes.

#### 4.2.2. Secondary magnetization

In this section we discuss the other obtained magnetization directions, presumably of secondary origin, for dykes outcropping *in situ*. In Chapada Diamantina, samples from *in situ* site S10B have a blood-red color, and appear weathered despite the fact that the samples were collected in relatively fresh river outcrops. These samples show NNE directed declinations with intermediate upward inclinations. This is broadly similar to the direction of the present Earth's magnetic field ( $D = 337.7^\circ$ ,  $I = -32.4^\circ$ ) at the sampling site, and we interpret it as a recent chemical/crystallization remagnetization. Further support for the weathering induced remagnetization comes from low-temperature remanence measurements that reveal presence of goethite in samples from this site and from thermomagnetic analyses (Fig. 4). The heavily weathered sill at site S10F shows N declination and intermediate downward pointing inclinations, with unblocking temperatures of  $\sim 500$  °C. These results are not included in the mean pole because of the poor statistics. At site S10C a 1-m-wide mafic dyke close to the city of Andaraí intrudes Tombador Formation (Fig. 2). The dyke shows NW steeply to intermediate downward ChRM that is significantly separated from the modal ChRM directional group, and is not included in the mean. Baked sandstone samples up to 0.18 m from the mafic dyke show northerly and shallower directions, indicating a negative baked contact test. Our northerly-downward results from these sites are broadly similar to Early-Middle Cambrian overprint directions recognized in Neoproterozoic carbonates of the Chapada Diamantina area (D'Agrella-Filho et al., 2000; Trindade et al., 2004), and we suspect these directions represent local overprinting in our study as well.

In Curaçá the dated weathered *in situ* part of the dyke S11CU shows southwest shallow up direction. Similar direction has been obtained earlier from two outcrops from the coastal Bahia areas: from the Itaju do Colônia suite (D'Agrella-Filho et al., 1990) and from one amphibolite outcrop at the coast of Olivença (Evans et al., 2016b) where it has been explained by local hydrothermal overprinting during the Brasiliano (late Neoproterozoic-Cambrian) orogeny. Samples from the *in situ* dyke S11CR (Poço de Fora) show SSE

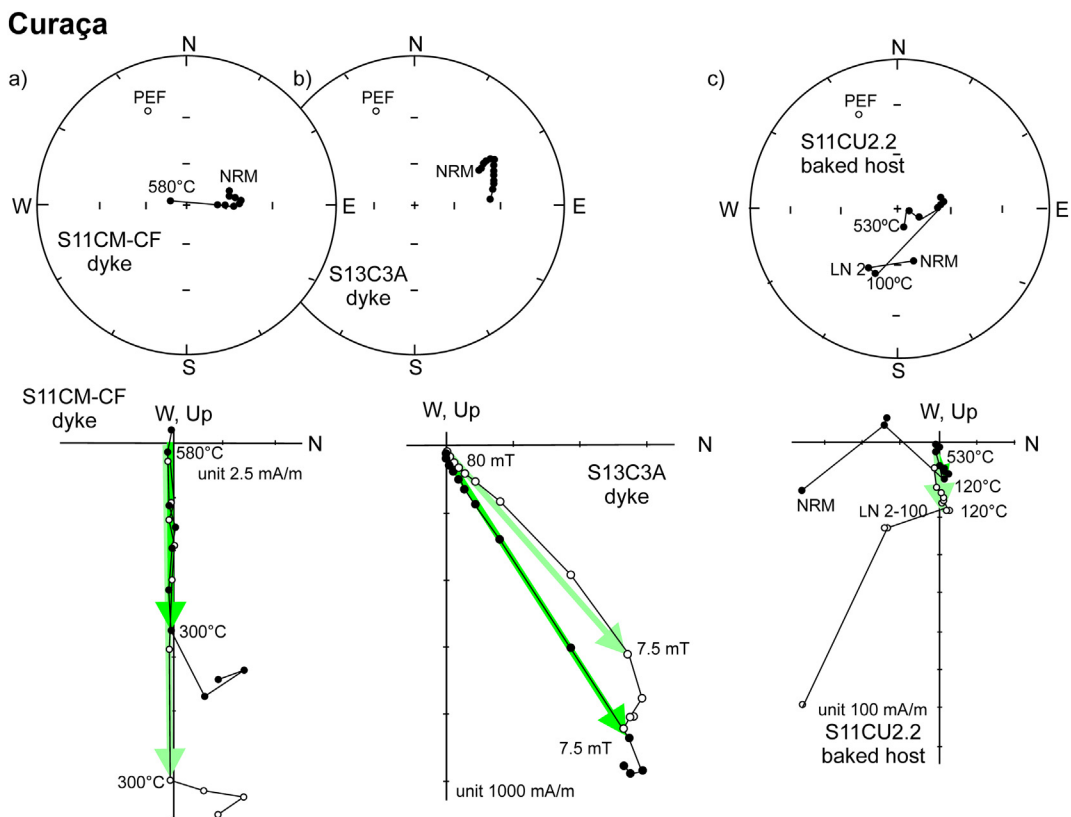


**Fig. 7.** Examples of Curaçá palaeomagnetic data. Demagnetization data for (a) the dyke S11CM, (b) the dyke S13C3, and (c) the baked host for dated ( $1506.7 \pm 6.9$  Ma; Silveira et al. (2013)) dyke S11CU. Green arrows indicate 1.5 Ga characteristic remanence direction. Symbols as in Fig. 6. (For interpretation of the references to colour in this figure legend, the reader is referred to the web version of this article.)

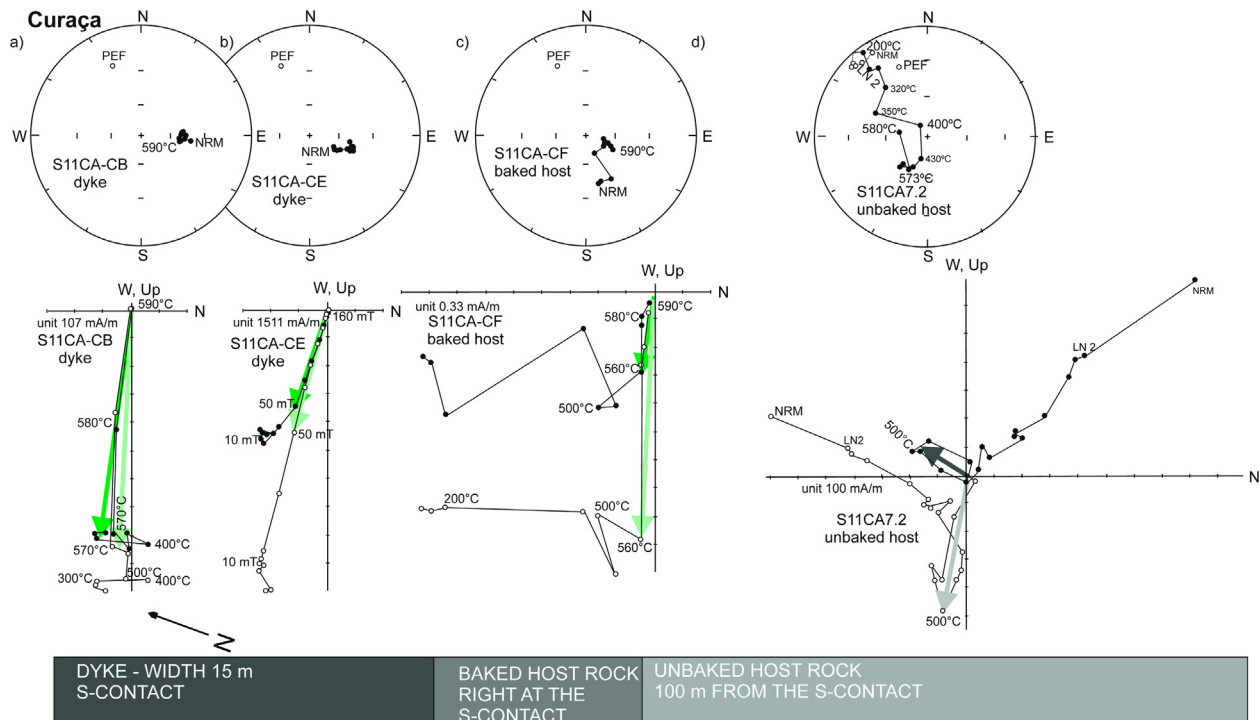


**Fig. 8.** Positive baked contact test for Curaçá dyke S11CA. Representative demagnetization data (a) and (b) for dyke S11CA, (c) for a baked host sample for the dyke S11CA, (d) for unbaked host for the dyke S11CA. Symbols as in Fig. 6.

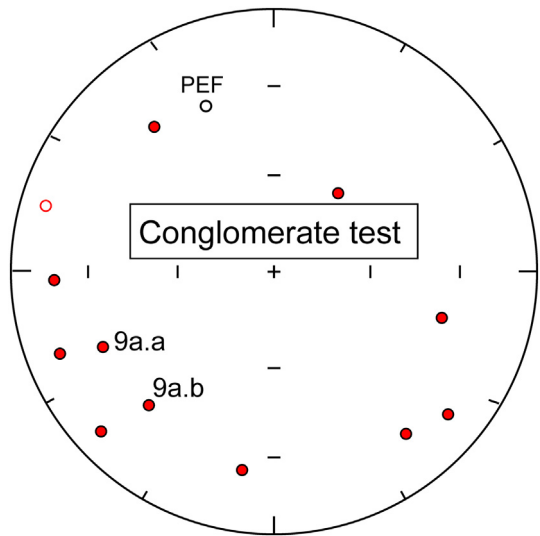


**Fig. 9.** An equal-area projection showing the ChRM directions in 11 mafic clasts in a conglomerate from Chapada Diamantina region. ChRMs of different clasts show randomly oriented directions and therefore pass the conglomerate test. The doubly sampled clast #9a is identified to show internal consistency of its ChRM.

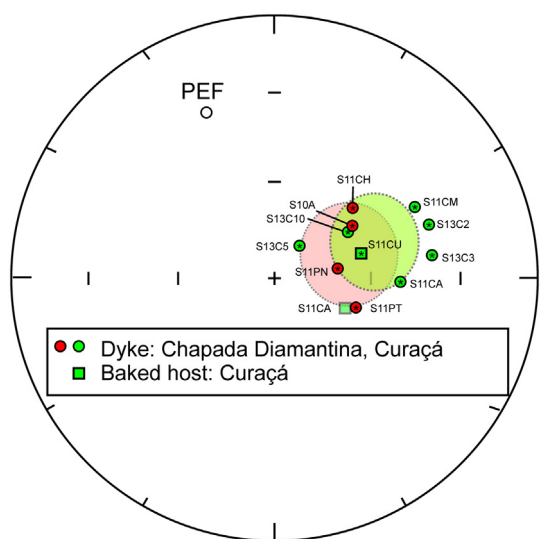


**Fig. 10.** Site mean directions for primary remanent magnetization for Chapada Diamantina and Curaçá dykes and their host rocks (see Table 1). Closed symbols represent downward directions. Dark color and \* – included in the mean calculation. Transparent color – not included in the mean. PEF – Present Earth's Field direction at sampling sites. Light red – mean of Chapada Diamantina. Light green – mean of Curaçá. (For interpretation of the references to colour in this figure legend, the reader is referred to the web version of this article.)

declinations with shallow to intermediate downward inclinations. A similar direction is obtained from baked host rock samples from this site. The direction is not seen in other sites of this study, and is interpreted here to represent a geomagnetic excursion at ca. 1500 Ma. That dyke is not dated directly, however, so it could be part of a swarm of substantially different age.

## 5. Discussion

### 5.1. Apparent polar wander path of the Congo/São Francisco/

New paleomagnetic data for dated Curaçá dykes ( $1506.7 \pm 6.9$  Ma; Silveira et al., 2013), with a positive baked contact test

reported herein, add to the low number of reliable Precambrian paleomagnetic poles for C/SF craton. The new ca. 1500 Ma pole is close to that of the ca. 2.0 Ga ( $^{40}\text{Ar}$ - $^{39}\text{Ar}$  plateau ages of  $2035 \pm 4$  Ma on hornblende and  $1876 \pm 4$  Ma on biotite) Jequié charnockite pole from the São Francisco craton (D'Agrella-Filho et al., 2011), but it also plots close to Early-Middle Cambrian poles (ca. 510 Ma) from across Gondwana (Fig. 11; McElhinny et al., 2003; Trindade et al., 2004; Mitchell et al., 2010). Three "Brasiliiano" mountain belts surround the São Francisco craton: the Brasília belt to the west, the Araçai belt to the east, and the Riacho do Pontal-Sergipano belt to the north (Fig. 1). In all of them, peak metamorphic conditions were attained before 550 Ma ago (Brito Neves et al., 1999; Oliveira et al., 2010), but remagnetization by low-temperature hydrothermal fluids in the cratonic foreland may have persisted well into Early Cambrian time (Trindade et al., 2004). Nonetheless, the mean dyke ChRM remains distinct from that north-down remagnetization direction, as noted above; and the positive baked contact test on a Curaçá dyke precludes a Cambrian remagnetization of our study area. Chapada Diamantina pole of unknown age plots in-between Jequié charnockite and Curaçá poles.

In addition to the new Curaçá pole there are only two other Precambrian poles with a positive field test and well-defined age from C/SF: the recent pole from 920 Ma Bahia coastal dykes (Evans et al., 2016b) for SF, and the pole for  $2680 \pm 10$  Ma Nyanzian lavas from Tanzania (Meert et al., 1994b). We have listed the existing >900 Ma Precambrian paleomagnetic data for C/SF in Table 2, showing also Van der Voo (1990) grading: (1) Well-determined rock age and a, modified to exclude criterion #7, which is ambiguous and subjective presumption that magnetization is the same age; (2) Sufficient number of samples ( $N > 24$ ),  $k$  (or  $K$ )  $\geq 10$  and  $\alpha_{95}(A_{95}) \leq 16^\circ$ ; (3) Adequate demagnetization procedure that demonstrably includes vector subtraction; (4) Field tests that constrain the age of magnetization; (5) Structural control and tectonic coherence with the craton or block involved; (6) The presence of reversals; and (7) No resemblance to paleopoles of younger age. There are other poles for ages younger than 900 Ma (e.g., Meert et al., 1995; Moloto-A-Kenguema et al., 2008) that are not listed in the Table 2.

There are three Neoarchean-Paleoproterozoic poles relevant to the paleogeographic analysis in this study (Fig. 11): the  $2680 \pm 10$  Ma key pole from Nyanzian lavas in Kenya (Meert et al., 1994b) on Tanzanian craton; the  $2623.8 \pm 7.0$  Ma (U-Pb; Oliveira et al., 2013) pole from Uauá tholeiitic mafic dykes in SF (D'Agrella-Filho and Pacca, 1998) lacking positive field stability tests; and the 2.03 Ga pole from the Jequié charnockites in SF (D'Agrella-Filho et al., 2011) that also lacks positive field stability tests, but shows reversals (Table 2, Fig. 11). For the Jequié charnockites,  $^{40}\text{Ar}$ - $^{39}\text{Ar}$  plateau ages of  $2035 \pm 4$  Ma (hornblende) and  $1876 \pm 4$  Ma (biotite) have been published (D'Agrella-Filho et al., 2011).

There are three Mesoproterozoic paleomagnetic poles for C/SF. The pole from the Late Kibaran intrusives from Congo (Meert et al., 1994a) does not have positive field tests and has large age uncertainties ( $1236 \pm 24$  Ma from  $^{40}\text{Ar}$ - $^{39}\text{Ar}$ , ibid.; ca. 1400–1375 Ma from U-Pb, Maier et al., 2007; Tack et al., 2010). The pole from Kunene Anorthosite complex for Congo (Piper, 1974) has well determined rock ages of  $1371 \pm 2.5$  Ma (U-Pb zircon in mangerite, Mayer et al., 2004),  $1376 \pm 2$  Ma (U-Pb zircon in syenodiorite, Drüppel et al., 2007) and  $1363 \pm 17$  Ma (U-Pb baddeleyite in gabbroic anorthosite, Maier et al., 2013), but does not have adequate statistics or methods used for demagnetization; nonetheless, paleomagnetic data does show two polarities. Our new pole for Curaçá dykes for SF is of high quality, with well-determined rock age of  $1506.7 \pm 6.9$  Ma (U-Pb baddeleyite, Silveira et al., 2013), adequate statistics, obtained with modern laboratory and analytical methods, and showing a positive baked contact test (Table 2, Fig. 11).

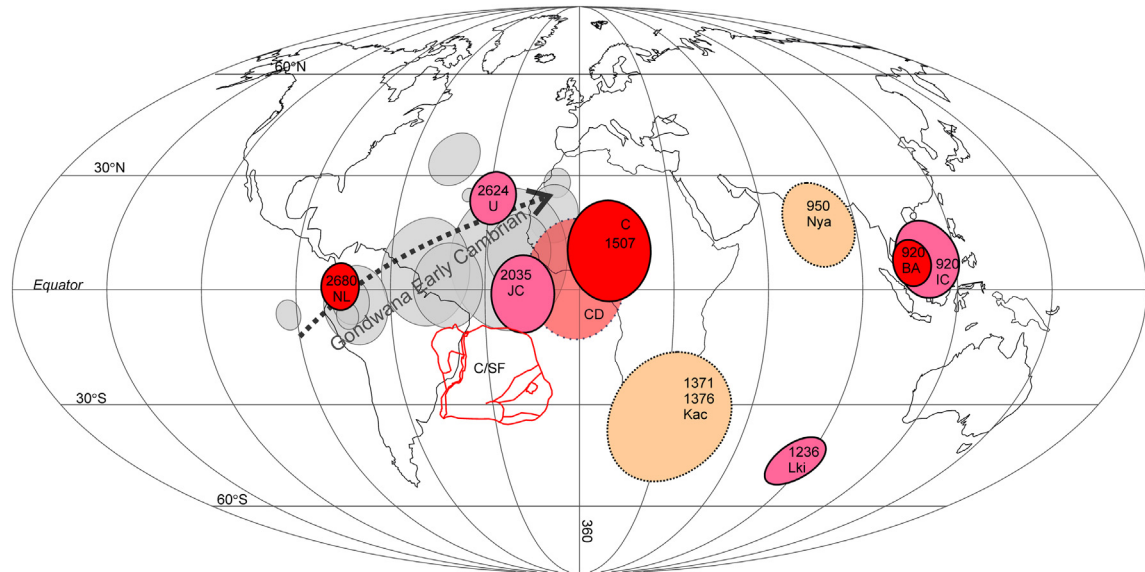


**Fig. 11.** Paleomagnetic poles from the C/SF craton and C/SF craton (red outlines) in present South American coordinates (Table 2). Pole colors: dark red – Van der Voo criteria  $> 5$ ; pink – Van der Voo criteria = 4 or 3; pale and dotted line – Van der Voo criteria = 2; and grey – paleomagnetic poles of Gondwana (Mitchell et al., 2010). Poles from this study: Chapada Diamantina (CD) shown with transparent color and Curaçá (C) shown with dark color. Numbers are ages in Ma. Pole abbreviations match those in Table 2. Arrow indicates the progression of ages of Gondwana poles. (For interpretation of the references to colour in this figure legend, the reader is referred to the web version of this article.)

**Table 2**

Paleoproterozoic to Early Neoproterozoic paleomagnetic poles for Congo/São Francisco.

Rock unit	Code	Age(Ma)	Method	Lat °N	Long °E	$A_{95}(\circ)$	123456	$Q_{(6)}$	Paleomagnetic Reference	Geochronology Reference
<i>São Francisco/Congo</i>										
Bahia coastal A (2-polar.)	BA	ca. 920	U-Pb	07	106	6	111111	6	Evans et al. (2016b)	Evans et al. (2016b), Renne et al. (1990)
Itaju do Colônia	IC	ca. 920?	Correl.	08	111	10	011011	4	D’Agrella-Filho et al. (1990)	Evans et al. (2016b)
Nyabikere pluton <sup>a</sup>	Nya	ca. 950?	Ar/Ar	17	078	11	101000	2	Meert et al. (1994a)	Meert et al. (1994a)
Late Kibaran Intrusives <sup>a</sup>	Lki	1236 ± 24	Combined	-46	086	7	111000	3	Meert et al. (1994a)	Meert et al. (1994a)
Kunene Anorthosite Complex <sup>a</sup>	Kac	1371 ± 2.5, 1376 ± 2	U-Pb						Piper (1974)	Mayer et al. (2004)
Curaçá dykes	C	1506.7 ± 6.9	U-Pb	10	010	15.8	111110	5	This work	Drüppel et al. (2007)
Jequié charnockites	JC	2035 ± 4	Ar/Ar	-01	342	10	011011	4	D’Agrella-Filho et al. (2011)	Silveira et al. (2013)
Uauá	U	2623.8 ± 7.0	U-Pb	24	331	7	111000	3	D’Agrella-Filho and Pacca (1998)	Oliveira et al. (2013)
Nyanzian lavas <sup>a</sup>	NL	2680 ± 10	U-Pb	0.9	284	6	11111	6	Meert et al. (1994b)	Meert et al. (1994b)

Notes: correl. = correlation of undated rocks to others in the table with direct age constraints. The  $^{40}\text{Ar}/^{39}\text{Ar}$  age on “reversed” dykes (Renne et al., 1990) is thus assumed as an approximate maximum constraint for that polarity. Code in Figs. 11.  $Q_{(6)}$  is Van der Voo (1990) grading, modified to exclude criterion #7, which is ambiguous and subjective.

<sup>a</sup> Rotated to São Francisco reference frame using Euler parameters ( $46.8^\circ$ ,  $329.4^\circ$ ,  $-55.9^\circ$ ) from McElhinny et al. (2003).

Recently, a high-quality Early Neoproterozoic 920 Ma (U-Pb) pole from Bahia coastal dykes in SF, with positive field test and well-determined rock age, was published (Evans et al., 2016b). The pole from Itaju do Colônia area in Bahia (D’Agrella-Filho et al., 1990) does not have a positive baked contact test or a well-determined rock age, but it generally agrees with the Bahia coastal dykes result and is presumably about the same age (Fig. 11). Neoproterozoic data from Itaju do Colônia show antiparallelism, whereas two-polarity data from Bahia coastal dykes do not. Only one other early Neoproterozoic pole exists from the C/SF craton; the Nyabikere pluton VGP from Congo craton (Meert et al., 1994a) derives from one site with no tilt control. No other localities bear the same “anomalous” direction, which is interpreted to represent a thermal overprint dated by  $^{40}\text{Ar}/^{39}\text{Ar}$  geochronology at ca. 950 Ma. In the São Francisco reference frame, the Nyabikere VGP (Table 2) is similar to the 920 Ma poles (Fig. 11).

We consider Precambrian motions of C/SF craton in terms of paleolatitudes and distances between paleomagnetic poles (Fig. 11) moving forward in time. Angular distance between the equatorial 2.68 Ga Nyanzian lavas pole (Congo craton in São Francisco reference frame) and the 2.62 Ga Uauá pole (SF) is ca.  $50^\circ$ , and it is possibly that the C/SF craton was not amalgamated before Paleoproterozoic time. The 2.04 Ga Jequié pole indicates high paleolatitude of the supercraton “Atlantica” (Rapalini et al., 2015). Although our new 1.5 Ga pole from Curaçá regions is proximal to the Jequié pole, we suspect the possibility of substantial APW in the intervening half billion years, that is simply not yet represented by reliable C/SF paleomagnetic data. After that, the ca. 1370 Ma Kunene Anorthosite complex pole and the Late Kibaran pole in the SF reference frame, if proven to be reliable, would indicate a substantial APW track showing migration of C/SF to low paleolatitudes. Thereafter, early Neoproterozoic data

**Table 3**

Selected 1.7–1.3 Ga paleomagnetic poles for testing the extended core of Nuna supercontinent.

Code	Rock unit	Plat (°N)	Plong (°E)	A <sub>95</sub> (°)	123456	Q <sub>(6)</sub>	Age (Ma)	References
BALTICA-FENNOSCANDIA								
H	Hötöng babbro	43.0	233.3	10.9	111100	4	1786 ± 3.0	Elming et al. (2009)
Sm	Småland intrusives	45.7	182.8	8.0	111111	6	1780 ± 3, 1776 +8/-7	Pisarevsky and Bylund (2010)
Si	Sipo Quartz porphyry dykes	26.4	180.6	9.4	111010	4	1633 ± 10	Mertanen and Pesonen (1995)
Qpr	Quartz porphyry dykes	30.2	175.4	9.4	101010	3	1631	Neuvonen (1986)
A	Åland dykes	23.7	191.4	2.8	111111	6	1575.9 ± 3.0	Salminen et al. (2016)
SK	Satakunta N-S and NE-SW dykes	29.3	188.1	6.6	111111	6	1575.9 ± 3.0	Salminen et al. (2014, 2016)
B-G	Bunkris-Glysjön-Öje dykes	28.3	179.8	13.2	101010	3	1461	Pisarevsky et al. (2014)
L	Lake Ladoga mafic rocks	11.8	173.3	7.4	111111	6	1457	Salminen and Pesonen (2007), Shcherbakova et al. (2008), Pisarevsky et al. (2013)
PJ2	Post Jotnian intrusions	4.0	158.0	4.0	111110	5	1265	Pesonen et al. (2003)
PJ1	Post Jotnian intrusions	-1.8	159.1	3.4	111110	5	1265	Pisarevsky et al. (2013)
AMAZONIA								
Av	Avanavero mafic rocks	48.4	207.5	9.2	111110	5	1785.5 ± 2.5	Bispo-Santos et al. (2014); Reis et al. (2013)
CV	Colider volcanics	63.3	118.8	11.4	111011	5	1785	Bispo-Santos et al. (2008)
SC	Salto do Ceu mafic intrusions	56.9	081.5	7.9	111111	6	1439	D'Agrella-Filho et al. (2016)
NG	Nova Guarita dykes	47.9	065.9	7.0	111111	6	1418.5 ± 3.5	Bispo-Santos et al. (2012)
I	Indiaivai gabbro	57.0	069.7	8.9	111000	3	1416	D'Agrella-Filho et al. (2012)
LAURENTIA+ GREENLAND								
Cl	Cleaver dykes	19.4	276.7	6.1	111110	5	1740	Irving et al. (2004)
MB	Melville Bugt dykes	5.0	274.0	9.0	111011	5	1622 + 3, 1635 + 3	Halls et al. (2011)
WCD	Western Channel diabase dykes	09.0	245.0	7.0	111010	4	1592 ± 3	Irving et al. (1972)
							1590 ± 4	Hamilton and Buchan (2010)
St.F	St. Francois Mnt acidic rocks	-13.2	219.0	6.1	111110	5	1476 ± 16	Meert and Stuckey (2002)
MIC	Michikamau intrusion	-01.5	217.5	4.7	111101	5	1460 ± 5	Emslie et al. (1976)
R.Mnt	Mean Rocky Mnt intrusion	-11.9	217.4	9.7	111001	4	1430	Elming and Pesonen (2010)
PL	Purcell lava	-23.6	215.6	4.8	111110	5	1443	Elston et al. (2002)
Sp	Spokane Fm	-24.8	215.5	4.7	111110	5	1457	Elston et al. (2002)
ZZ	Zig-Zag Dal intrusions	11.0	221.0	3.0	111010	4	1382 ± 2	Evans and Mitchell (2011)
MK	Mackenzie dykes	4.0	190.0	5.0	111110	5	1267+7/-3	Buchan and Halls (1990)
S	Sudbury dykes	-2.5	192.8	2.5	111110	5	1237	Palmer et al. (1977)
SIBERIA								
K	Kuonamka dykes	06.0	234.0	19.8	101011	4	1503 ± 5	Ernst et al. (2000)
W.An	West Anabar intrusions	25.3	241.4	4.6	111110	5	150 ± 2	Evans et al. (2016a)
N.An	North Anabar intrusions	23.9	255.3	7.5	111010	4	1483 ± 17	Evans et al. (2016a)
SoKy	Sololi - Kyutinge intrusions	33.6	253.1	10.4	111110	5	1473 ± 24	Wingate et al. (2009)
Ch	Chieress dykes	05.0	258.0	6.7	101010	3	1384 ± 2	Ernst and Buchan (2000)
CONGO-SF								
C	Curaçá dykes <sup>b</sup>	41.6	041.4	15.8	111110	5	1506.7 ± 6.9	This work
Kac	Kunene Anorthosite complex	03.3	075.3	18.0	100001	2	1371 ± 2.5, 1376 ± 2	Piper (1974)

Code – code in Figs. 11 and 13; Plat – pole latitude; Plong – pole longitude; A95 – 95% confidence circle of the pole. Q<sub>(6)</sub> is Van der Voo (1990) grading, modified to exclude criterion #7, which is ambiguous and subjective.

<sup>b</sup> São Francisco rotated to Congo reference frame using Euler parameters (46.8°, 329.4°, +055.9°) from McElhinny et al. (2003).

**Table 4**Euler rotation poles (Elat, Elong, E<sub>rot</sub>) for Nuna reconstruction at 1500 Ma.

From-to	E <sub>lat</sub> , E <sub>long</sub> , E <sub>rot</sub>	Reference
Laurentia to grid	38.8°, -151.4°, +159.7°	This study interpolating between Laurentia poles (Western Channel Diabase, St Francois Mountains)
Baltica to Laurentia	47.5°, 001.5°, +49.0°	Evans and Pisarevsky (2008)
Siberia-Aldan to Siberia-Anabar	60°, 115°, +25°	Evans (2009)
Siberia-Anabar to Laurentia	77°, 98°, +137°	Evans et al. (2016a)
Amazon to Baltica	62.97°, -111.66°, +90.42°	This study option A
Amazon to Laurentia	52.43°, -76.67°, +108.68°	This study option A
Congo to Laurentia	-22.7°, -133.75°, -207.72°	This study option A
Amazon to Baltica	35.0°, -90.5°, +107.2°	This study option B
Amazon to Laurentia	25.57°, -64.21°, 132.51°	This study option B
Congo to Laurentia	-23.35°, -142.67°, -196.87°	This study option B
São Francisco to Congo	46.8°, 329.4°, +055.9°	McElhinny et al. (2003)

indicate a return of C/SF to moderate-high paleolatitude by 920 Ma.

### 5.2. Implications for Nuna

There is a consensus that Baltica and Laurentia form the core of the Nuna supercontinent in the geologically and paleomagnetically

viable North Europe North America (NENA; Gower et al., 1990) connection where northern Norway and Kola Peninsula of Baltica are facing northeastern Greenland of Laurentia (Fig. 12) between ca. 1.75 and ca. 1.27 Ga (Salminen and Pesonen, 2007; Evans and Pisarevsky, 2008; Lubnina et al., 2010; Pisarevsky and Bylund, 2010; Evans and Mitchell, 2011), but see also different suggestions of Johansson (2009) and Halls et al. (2011). Recently, based on

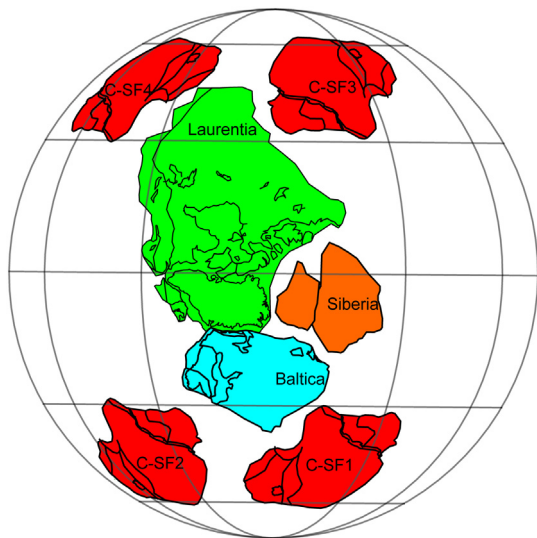


**Fig. 12.** Plausible (partial) Nuna reconstructions at 1.5 Ga including the Congo/São Francisco craton (red), using the Curaçá pole of this study. Baltica (blue) and Laurentia (green) are restored in the NENA configuration (Gower et al., 1990) using the Euler parameters of Evans and Pisarevsky (2008). Siberia (orange) in tight-fit with Laurentia based on recent data from Anabar (Pavlov et al., 2014; Evans et al., 2016a,b). Grid lines are 30°, and absolute paleolongitude is arbitrary. Euler rotations are listed in Table 4. (For interpretation of the references to colour in this figure legend, the reader is referred to the web version of this article.)

Mesoproterozoic passive margins surrounding Siberia (Pisarevsky and Natapov, 2003) and similar geology between Siberia and Western Greenland from 1.9 Ga on, it was proposed that Siberia forms the Nuna core together with Baltica and Laurentia in tight fit between East Siberia and Western Greenland (e.g. Rainbird et al., 1998; Wu et al., 2005; Evans and Mitchell, 2011; Ernst et al.,

2016; Evans et al., 2016a). This tight fit of Baltica, Laurentia and Siberia forming the core of Nuna is supported by 1.8–1.38 Ga paleomagnetic data from these continents, but see for an alternative view of Siberia's loose fit with Laurentia in Pisarevsky et al. (2008).

This is the first time that the position of Congo/São Francisco craton at 1.5 Ga is reconstructed using paleomagnetic data. In Fig. 12, a range of possible reconstructions of C/SF craton with the core of Nuna is shown, based on  $1506.7 \pm 6.9$  Ma paleomagnetic pole from Curaçá dykes, and exercising freedom of both paleolongitude and geomagnetic polarity. The new 1.5 Ga paleomagnetic data restore C/SF to moderate paleolatitudes. Based on coeval 1.5 Ga magmatism in Baltica, Siberia and C/SF, we favor the position C-SF1, where SW Congo is reconstructed against S-SE Baltica. This is supported also by the coeval 1.38 Ga magmatism in Congo craton (Kunene anorthosite complex; Piper, 1974; Mayer et al., 2004; Drüppel et al., 2007; Maier et al., 2013), SE-E Baltica in the Volgo Uralian region (Mashak event; Puchkov et al., 2013), and in the eastern Anabar shield in Siberia (Chieress dykes, Ernst et al., 2000). In our reconstructions the Siberian craton is first restored to its configuration prior to ~20–25° Devonian rotation in the Vilyuy graben (Pavlov et al., 2008; Evans, 2009; Table 4).

The new pole from C/SF is used to reconstruct an extended core of Nuna at 1.5 Ga, with Baltica, Laurentia, Siberia, and Amazonia. There are not enough high-quality Mesoproterozoic paleomagnetic poles to construct adequate APWPs for different cratons that could be used to test the assembly of Nuna (Pisarevsky et al., 2014). It is therefore necessary to rely primarily on the “key pole” comparisons (Buchan et al., 2000; Buchan, 2013), which causes additional problems such as polarity ambiguity and longitudinal uncertainty. Although those problems can be partly resolved by comparison of coeval paleopoles from different continents (Cawood et al., 2006; Evans and Pisarevsky, 2008), there are very few coeval key-pole pairs available (Table 3). Our discussion of possible pole/age comparisons relies on the global compilations of paleomagnetic data by Nordic Paleomagnetic Workshops in Haraldsvangen (Norway) in

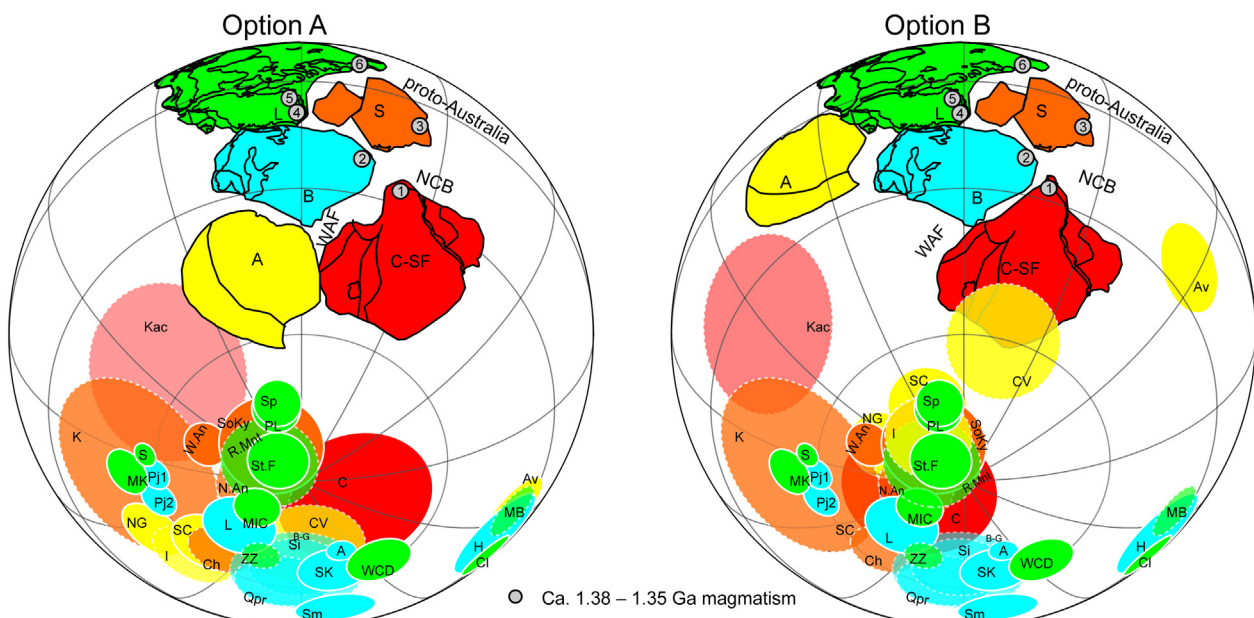


**Fig. 13.** Plausible reconstructions on the extended core of Nuna at 1500 Ma including Baltica (B, blue), Laurentia (L, green), Siberia (S, orange), Congo/São Francisco (C/SF, red), and Amazonia (A, yellow). Poles, listed in Table 3, are color-coded according to craton, shaded according to reliability (darker with solid outline = key pole), and rotated to the reconstructions presented. Used Euler rotations in Table 4. In both reconstructions, Laurentia and Baltica are shown in the NENA configuration (Evans and Pisarevsky, 2008) and Siberia in a tight fit with Laurentia based on recent data from Anabar (Pavlov et al., 2014; Evans et al., 2016a). Options A and B are discussed in the text. Grid lines are 30° and absolute paleolongitude is arbitrary. Ca. 1.38–1.35 Ga magmatism; 1 Kunene anorthosite complex; 2 Mashak volcanics; 3 Chieress dyke; 4 Midsommerso sills and Zig Zag volcanics; 5 Victoria Land dykes; and 6 Hart River sill. WAF West Africa; NCB North China Block. (For interpretation of the references to colour in this figure legend, the reader is referred to the web version of this article.)

2014. In general, very few data exist for ca. 1500 Ma and for the interval of relevance to our new results. There is not a good quality 1500 Ma paleomagnetic data for Baltica for direct comparison to our new C/SF pole. The existing pole for  $1505 \pm 8$  Ma Rödö basic dykes (Moakhar and Elming, 2000) fails to show positive field stability, and the  $1514 \pm 5$  Ma,  $1505 \pm 12$  Ma pole for Ragunda rapakiwi formation (Piper, 1979; Persson, 1999) fails to show positive field stability test and magnetization resembles the well known NE intermediately downward remagnetization direction widely obtained across Fennoscandia (e.g. Salminen et al., 2014; 2016; submitted). Regardless, the presence of 1.5 Ga magmatism in Baltica adds one LIP record for Baltica, making it similar to C/SF, which could indicate the close neighborhood of these cratons. Moreover, for Baltica there are other high quality Mesoproterozoic paleomagnetic data (see Table 3) for reconstructing the paleogeography of the core of Nuna. For Laurentia there are many high-quality Mesoproterozoic paleomagnetic poles (Table 3). The 1.5 Ga reconstruction of Laurentia for this study is made by interpolating between Western Channel Diabase ( $1592 \pm 3$  Ma,  $1590 \pm 4$  Ma; Hamilton and Buchan, 2010) and St Francois Mountains. ( $1476 \pm 16$  Ma; Meert and Stuckey, 2002) poles (Figs. 12 and 13). Siberian high quality ca. 1.5 Ga paleomagnetic poles for West Anabar ( $1503 \pm 2$  Ma; Evans et al., 2016a) and for Sololi-Kyutingde ( $1473 \pm 24$  Ma; Wingate et al., 2009) support the tight fit between Baltica, Laurentia and Siberia (e.g. Rainbird et al., 1998; Evans and Mitchell, 2011; Pavlov et al., 2014; Evans et al., 2016a) and proximity of C/SF and Siberia. The alternative looser fit between Laurentia and Siberia (Pisarevsky and Natapov, 2003; Pisarevsky et al., 2008) poses no difficulty with our reconstruction model of C/SF.

In this study we show two reconstruction options for Amazonia against Baltica. In our option A, North Amazonia is facing South Baltica close to the SAMBA fit (Johansson, 2009) so that the 1900–1850 Ma Svecofennian orogeny in Baltica continues into the 1980–1810 Ma Ventuari-Tapajós province in Amazonia, and the 1850–1650 Ma Transscandinavian igneous belt and the 1640–1520 Ma Gothian orogeny have their continuation into the 1780–1550 Ma Rio Negro-Juruena province. The ca. 1.79 Ma Colider volcanics paleopole (Bispo-Santos et al., 2008) does not support this fit. However, the more recent ca. 1.79 Ga Avanavero key paleopole (Bispo-Santos et al., 2014) of Amazonia and the 1.79 Ga Hötting gabbro pole from Baltica support option A, as do ca. 1.4 Ga Salto do Ceu, Indiavaí and Nova Guarita poles of Amazonia (Bispo-Santos et al., 2012; D'Agrella-Filho et al., 2016) and ca. 1.4 Ga poles from Baltica. In the option B, South Amazonia is reconstructed to West Baltica so that Late Mesoproterozoic-Early Neoproterozoic Sunas orogeny has a direct eastward continuation into the coeval Sveconorwegian orogeny. This is supported by ca. 1.4 Ga poles from both continents, but not by older poles (e.g., Avanavero vs. Hötting), requiring that Amazonia and Baltica assembled into the option B configuration between 1.8 and 1.4 Ga. Full geological evaluation of option B is beyond the scope of this paper, but we note the existence of 1.6–1.5 Ga Labradorian and Pinwarian tectonic events in the northern Grenville Province of eastern Canada (e.g., Heaman et al., 2004) and Gothian tectonism in Scandinavia (Åhall and Connelly, 2008), which could document arrival of Amazonia at that time (could it perhaps be the large tectonic backstop to the “Proto SW Norway” terrane inferred in the latter paper?). Absence of widespread 1.5 Ga tectonism in eastern Amazonia could be explained by a lower-plate setting for that side of the craton during its accretion to Nuna, although the subduction polarity would need to have switched along strike to the south (Geraldes et al., 2001), similar to Cenozoic tectonics of the Alpine-Ligurian region (Argnani, 2012). We do not explicitly show West Africa in our reconstructions (Fig. 13), since there are no reliable Mesoproterozoic paleomagnetic data for that craton. There is room for West

Africa in both of the shown options, although not in typical SAMBA or Gondwana configurations (Trompette, 1994; Johansson, 2009).

The reconstruction of C/SF at 1.5 Ga is only slightly different between the options A and B (Fig. 13), and neither of these allow the recently proposed tight fit of Siberian and East São Francisco craton between 1.5 and 1.38 Ga (Ernst et al., 2013; Silveira et al., 2013; Pisarevsky et al., 2014), but they do allow the close proximity of Siberia and SW Congo craton. Option B conforms better to our new paleomagnetic data for C/SF and brings C/SF closer to Baltica than in option A. We have plotted the 1.38 Ga pole from Kunene anorthosite complex in Fig. 13, and it is not similar to 1.38 Ga poles from other cratons either option, but due to that pole's low quality we cannot exclude the continuation of either fit at 1.38 Ga. Both of the C/SF juxtapositions with Baltica are incompatible with paleomagnetic data from those cratons at 920 Ma (Evans et al., 2016b), indicating their separation during late Mesoproterozoic time. However, we are currently unable to test the duration of either configuration option more precisely.

## 6. Conclusions

A new, high-quality paleomagnetic pole for C/SF craton was obtained from  $1506.7 \pm 6.9$  Ma mafic dykes from Curaçá regions in Brazil. This pole reconstructs C/SF craton to mid-latitudes during the Nuna interval. Based on coeval 1.5 Ga and 1.38 Ga magmatism in Baltica, Siberia and C/SF, we favor the position where SW Congo is reconstructed against S-SE Baltica. We propose two optional reconstructions of the extended core of Nuna at 1500 Ma. In both of them Baltica, Laurentia and Siberia are reconstructed as discussed above, but the positions of Amazonia and C/SF vary. In option A, the more traditional fit of Amazonia with Baltica is shown, slightly differing from the geologically based SAMBA model of Johansson (2009). Amazonia's and Baltica's 1.78 Ga and ca. 1.4 Ga paleopoles support this fit. Our new paleomagnetic data for C/SF fits better with option B, but that model requires an unconventional dynamic reconstruction of south Amazonia to west Baltica. Option B is supported by ca. 1.4 Ga poles from both continents, but not with ca. 1.8 Ga poles – indicating that Amazonia and Baltica collided at some intervening time. In both options, SW Congo is reconstructed against S-SE Baltica, but in option A there is a gap in between Baltica and C/SF whereas in option B there is a tight fit between them. We are not able to test paleomagnetically the lifecycle of this fit due to lack and poor quality of later Mesoproterozoic C/SF poles.

## Acknowledgments

We thank Dr Paulo Donatti-Filho and Ms Florence Loi for their help at the field. JS was funded by Academy of Finland and Alfred Kordelin Foundation. GPlates software (<http://www.ccsf.mq.edu.au>) was used for paleogeographical reconstructions. EP and AS were supported by NSF (EAR-1149434). RIFT was supported by a Brazilian CNPq grant (304934/2014-3). EPO was supported by a Brazilian CNPq grant (305658/2015-8). This publication contributes to IGCP648 Supercontinent Cycles & Global Geodynamics.

## References

- Åhall, K.-I., Connelly, J.N., 2008. Long-term convergence along SW Fennoscandia: 330 m.y. of Proterozoic crustal growth. *Precambr. Res.* 161, 452–474.
- Alkmim, F.F., Brito Neves, B.B., Alves, J.A.C., 1993. Arcabouço tectônico do Cráton do São Francisco – uma revisão. In: Dominguez, J.M.L., Misi, A. (Eds.), O Cráton do São Francisco. Sociedade Brasileira de Geologia, Salvador, pp. 45–62.
- Alkmim, F.F., Marshak, S., Pedrosa-Soares, A.C., Peres, G.G., Cruz, S.C.P., Whittington, A., 2006. Kinematic evolution of the Araçuaí-West Congo in Brazil and Africa: nutcracker tectonics during the Neoproterozoic assembly of Gondwana. *Precambr. Res.* 149, 43–64.

- Argnani, A., 2012. Plate motion and the evolution of Alpine Corsica and Northern Apennines. *Tectonophysics* 579, 207–219.
- Babinski, M., Van Schmus, W.R., Chemale Jr., F., Brito Neves, B.B., Rocha, A.J.D., 1993. Idade isocrônica Pb/Pb em rochas carbonáticas da Formação Caboclo, em Morro do Chapéu. In: Simpósio do Craton do São Francisco. Brazilian Geological Society, Salvador, pp. 160–163.
- Babinski, M., Brito-Neves, B.B., Machado, N., Noce, C.M., Uhlein, A., Van Schmus, W.R., 1994. Problemas na metodologia U/Pb em zircões de vulcânicas continentais: o caso do Grupo Rio dos Remédios, Supergrupo Espinhaço, no estado da Bahia. *Boletim de Resumos Expandidos, SBG, Congresso Brasileiro de Geologia* 2, 409–410.
- Babinski, M., Pedreira, A.J., Brito Neves, B.B., Van Schmus, W.R., 1999. Contribuição à Geocronologia da Chapada Diamantina, VII Simpósio Nacional de Estudos Tectônicos, Lençóis, 118–120.
- Barbosa, J.S.F., Sabaté, P., 2004. Archean and Paleoproterozoic crust of the São Francisco Craton, Bahia, Brazil: geodynamic features. *Precambr. Res.* 133, 1–27.
- Barbosa, J.S.F., Sabaté, P., Marinho, M.M., 2003. O Cráton do São Francisco na Bahia: Uma Síntese. *Revista Brasileira de Geociências* 31 (1), 3–6.
- Bastos Leal, L.R., 1992. Geocronologia Rb-Sr e K-Ar, evolução isotópica e implicações tectônicas dos enxames de diques maficos de Uauá e Vale do Rio Curaçá, Bahia. In: Resumo de Teses Revista Brasileira de Geociências 22 (3), 375.
- Bastos Leal, L.R., Teixeira, W., Bellieni, G., Petrini, R., Piccirillo, E.M., 1995. Geocronologia e geoquímica isotópica de Sr e Nd nos diques maficos do Curaçá Craton do São Francisco (Brasil): registro de um evento distensivo Neoproteorozoico associado à evolução da Faixa Colisional Sergipana. *Geochimica Brasiliensis* 9 (2), 141–159.
- Batillani, G.B., Gomes, N.S., Guerra, W.J., 2007. The occurrence of microdiamonds in Mesoproterozoic Chapada Diamantina intrusive rocks — Bahia/Brazil. *Ann. Brazilian Acad. Sci.* 79, 321–332.
- Batillani, G.B., Vasconcellos, P.M., Gomes, N.S., Guerra, W.J., 2005. Geochronological data of dykes and sills intruding Proterozoic sequences of the Tombador Formation, Bahia, Brazil, III Simpósio sobre o Cráton do São Francisco, Salvador, 139–142.
- Bispo-Santos, F., D'Agrella-Filho, M.S., Pacca, I.I.G., Janikian, L., Trindade, R.I.F., Elming, S.-Å., da Silva, J.A., Barros, M.A.S., Pinho, F.M.A.S., 2008. Columbia revisited: paleomagnetic results from the 1790 Ma colider volcanics (SW Amazonian Craton Brazil). *Precambr. Res.* 164, 40–49.
- Bispo-Santos, F., D'Agrella-Filho, M.S., Trindade, R.I.F., Elming, S.-Å., Janikian, L., Vasconcelos, P.M., Perillo, B.M., Pacca, I.I.G., da Silva, J.A., Barros, M.A.S., 2012. Tectonic implications of the 1419 Ma Nova Guarita mafic intrusives paleomagnetic pole (Amazonian Craton) on the longevity of Nuna. *Precambr. Res.* 196 (197), 1–22.
- Bispo-Santos, F., D'Agrella-Filho, M.S., Trindade, R.I., Janikian, L., Reis, N.J., 2014. Was there SAMBA in Columbia? Paleomagnetic evidence from 1790Ma Avanavero mafic sills (northern Amazonian Craton). *Precambr. Res.* 244, 139–155.
- Bleeker, W., Ernst, R., 2006. Short-lived mantle generated magmatic events and their dyke swarms: the key unlocking Earth's palaeogeographic record back to 2.6 Ga. In: Hanski, E., Mertanen, S., Rämö, T., Vuollo, J. (Eds.), *Dyke Swarms — Time Markers of Crustal Evolution*. Balkema Publishers, Rotterdam, A.A., pp. 3–26.
- Borradaile, G.J., Luca, K., Middleton, R.S., 2004. Low-temperature demagnetization isolates stable magnetic vector components in magnetite-bearing diabase. *Geophys. J. Int.* 157, 526–536.
- Brito Neves, B., Campos Neto, M.C., Fuck, R.A., 1999. From Rodinia to Western Gondwana: an approach to the Brasiliano-Pan African cycle and orogenic collage. *Episodes* 22, 155–166.
- Buchan, K.L., 2013. Key Paleomagnetic poles and their use in Proterozoic Continent and Supercontinent reconstructions: a review. *Precambr. Res.* 238, 93–110.
- Buchan, K.L., Halls, H.C., 1990. Palaeomagnetism of Proterozoic mafic dyke swarms of the Canadian shield. In: Parker, A.J., Rickwood, P.C., Tucker, D.H. (Eds.), *Mafic Dykes and Emplacement Mechanism*. Balkema, Rotterdam, pp. 209–230.
- Buchan, K.L., Mertanen, S., Park, R.G., Pesonen, L.J., Elming, S.A., Abrahamsen, N., Bylund, G., 2000. Comparing the drift of Laurentia and Baltica in the Proterozoic: the importance of key palaeomagnetic poles. *Tectonophysics* 319, 167–198.
- Cawood, P.A., Kröner, A., Pisarevsky, S., 2006. Precambrian plate tectonics: criteria and evidence. *GSA Today* 16, 4–11.
- Condie, K.C., 2004. Supercontinents and superplume events: distinguishing signals in the geologic record. *Phys. Earth Planet. Sci.* 146, 319–332.
- D'Agrella-Filho, M.S., Trindade, R.I.F., Tohver, E., Janikian, L., Teixeira, W., Hall, C., 2011. Paleomagnetism and 40Ar/39Ar geochronology of the high-grade metamorphic rocks of the Jequié block, São Francisco Craton: Atlantica, Ur and beyond. *Precambr. Res.* 185, 183–201.
- D'Agrella-Filho, M.S., Trindade, R.I., Queiroz, M.V., Meira, V.T., Janikian, L., Ruiz, A.S., Bispo-Santos, F., 2016. Reassessment of Aguapeí (Salto do Céu) paleomagnetic pole, Amazonian Craton and implications for Proterozoic supercontinents. *Precambr. Res.* 272, 1–17.
- D'Agrella-Filho, M.S., Pacca, I.G., 1998. Paleomagnetism of Paleoproterozoic mafic dyke swarm from the Uauá region, northeastern São Francisco Craton, Brazil: tectonic implications. *J. S. Am. Earth Sci.* 11, 23–33.
- D'Agrella-Filho, M.S., Babinski, M., Trindade, R.I.F., Van Schmus, W.R., Ernesto, M., 2000. Simultaneous remagnetization and U-Pb isotope resetting in Neoproterozoic carbonates of the São Francisco craton, Brazil. *Precambrian Research* 99, 179–196.
- D'Agrella-Filho, M.S., Pacca, I.G., Renne, P.R., Onstott, T.C., Teixeira, W., 1990. Paleomagnetism of Middle Proterozoic (1.01 to 1.08 Ga) mafic dykes in southeastern Bahia State – São Francisco Craton, Brazil. *Earth Planet. Sci. Lett.* 101, 332–348.
- D'Agrella-Filho, M.S., Trindade, R.I.F., Elming, S., Teixeira, W., Yokoyama, E., Tohver, E., Geraldès, M.C., Pacca, I.I.G., Barros, M.A.S., Ruiz, A.S., 2012. The 1420 Ma Indianaíva Mafic Intrusion (SW Amazonian Craton): Paleomagnetic results and implications for the Columbia supercontinent. *Gondwana Res.* 22, 956–973.
- Danderfer, A., De Waele, B., Pedreira, A.J., Nalini, H.A., 2009. New geochronological constraints on the geological evolution of Espinhaço basin within the São Francisco Craton – Brazil. *Precambr. Res.* 170, 116–128.
- de Waele, B., Fitzsimons, I.C.W., Wingate, M.T.D., Tembo, F., Mapani, B., Belousova, E.A., 2009. The geochronological framework of the Irumide Belt: a prolonged crustal history along the margin of the Bangweulu craton. *Am. J. Sci.* 309, 132–187.
- Deckart, K., Féraud, G., Marques, L.S., Bertrand, H., 1998. New time constraints on dyke swarms related to the Paraná-Etendeka magmatic province, and subsequent South Atlantic opening, southeastern Brazil. *J. Volcanol. Geoth. Res.* 80, 67–83.
- Dröppel, K., Littmann, S., Romer, R.L., Okrusch, M., 2007. Petrology and isotopic geochemistry of the Mesoproterozoic anorthosite and related rocks of the Kunene Intrusive Complex, NW Namibia. *Precambr. Res.* 156, 1–31.
- Elming, S.A., Moakhar, M.O., Laye, P., Donadini, F., 2009. Uplift deduced from remanent magnetization of a Proterozoic basic dyke and the baked country rock in the Hötöng area, Central Sweden: a palaeomagnetic and 40Ar/39Ar study. *Geophys. J. Int.* 179, 59–78.
- Elming, S.-Å., Pesonen, L.J., 2010. Recent developments in paleomagnetism and geomagnetism. Sixth Nordic paleomagnetic workshop, Luleå (Sweden), 15–22 September 2009. *EOS* 90 (51), 502.
- Elston, D.P., Enkin, R.J., Baker, J., Kisilevsky, D.K., 2002. Tightening the Belt: Paleomagnetic-stratigraphic constraints on deposition, correlation, and deformation of the Middle Proterozoic (ca. 1.4 Ga) Belt-Purcell Supergroup, United States and Canada. *Geol. Soc. Am. Bull.* 114, 619–638.
- Emslie, R.F., Irving, E., Park, J.K., 1976. Further paleomagnetic results from the Michikamau intrusion, Labrador. *Can. J. Earth Sci.* 13, 1052–1057.
- Ernst, R., Bleeker, W., 2010. Large igneous provinces (LIPs), giant dyke swarms, and mantle plumes: significance for breakup events within Canada and adjacent regions from 2.5 Ga to the Present. *Can. J. Earth Sci.* 47, 695–739.
- Ernst, R.E., Buchan, K.L., 2000. Integrated Palaeomagnetism and U-Pb geochronology of mafic dikes of the Eastern Anabar Shield. *J. Geology* 108, 381.
- Ernst, R.E., Buchan, K.L., Hamilton, M.A., Okrugin, A.V., Tomshin, M.D., 2000. Integrated paleomagnetism and U-Pb geochronology of mafic dikes of the Eastern Anabar shield region, Siberia: implications for Mesoproterozoic paleolatitude of Siberia and comparison with Laurentia. *J. Geology* 108, 381–401.
- Ernst, R.E., Hamilton, M.A., Söderlund, U., Hanes, J.A., Gladkochub, D.P., Okrugin, A.V., Kolotilina, T., Mekhonoshin, A.S., Bleeker, W., LeCheminant, A.N., Buchan, K.L., Chamberlain, K.R., Didenko, A.N., 2016. Long-lived connection between southern Siberia and northern Laurentia in the Proterozoic. *Nat. Geosci.* 9, 464–469.
- Ernst, R.E., Wingate, M.T.D., Buchan, K.L., Li, Z.X., 2008. Global record of 1600–700 Ma Large Igneous Provinces (LIPs): implications for the reconstruction of the proposed Nuna (Columbia) and Rodinia supercontinents. *Precambr. Res.* 160, 159–178.
- Ernst, R.E., Pereira, E., Hamilton, M.A., Pisarevsky, S.A., Rodrigues, J., Tassinari, C.C.G., Teixeira, W., Van-Dunem, V., 2013. Mesoproterozoic intraplate magmatic 'barcode' record of the Angola portion of the Congo Craton: newly dated magmatic events at 1500 and 1110 Ma and implications for Nuna (Columbia) supercontinent reconstructions. *Precambr. Res.* 230, 103–118.
- Evans, D.A.D., 2009. The palaeomagnetically viable, long-lived and all-inclusive Rodinia supercontinent reconstruction. In: Murphy, J.B., Keppe, J.D. and Hynes, A., (Eds.), *Ancient Orogenes and Modern Analogues*. Geological Society of London Special Publication, 327, 37–404.
- Evans, D.A.D., Mitchell, R.N., 2011. Assembly and breakup of the core of Paleoproterozoic-Mesoproterozoic supercontinent Nuna. *Geology* 39, 443–446.
- Evans, D.A.D., Pisarevsky, S.A., 2008. Plate tectonics on early Earth? Weighing the paleomagnetic evidence. In: When Did Plate Tectonics Begin on Planet Earth? The Geological Society of America Special Paper, 440, 249–263.
- Evans, D.A.D., Veselovsky, R., Petrov, P.Y., Shatsillo, A., Pavlov, V.E., 2016a. Paleomagnetism of Mesoproterozoic margins of the Anabar Shield: a hypothesized billion-year partnership of Siberia and northern Laurentia. *Precambr. Res.* 281, 639–655.
- Evans, D.A.D., Trindade, R.I.F., Catelani, E.L., D'Agrella-Filho, M.S., Heaman, L.M., Oliveira, E.P., Söderlund, U., Ernst, R.E., Smirnov, A.V., Salminen, J.M., 2016b. Return to Rodinia? Moderate to high paleolatitude of the São Francisco/Congo craton at 920 Ma. In: Li, Z. X., Evans, D.A.D. and Murphy, J.B. (Eds.), *Supercontinent Cycles Through Earth History*. Geological Society of London Special Publications, 424, 167–190.
- Everitt, C.W.F., Clegg, J.A., 1962. A field test of paleomagnetic stability. *Geophys. J. London* 6, 312–319.
- Fisher, R., 1953. Dispersion of a sphere. *Proc. Royal Soc. London* 217, 295–305.
- Geraldès, M.C., Van Schmus, W.R., Condie, K.C., Bell, S., Teixeira, W., Babinski, M., 2001. Proterozoic geologic evolution of the SW part of the Amazonian Craton in Mato Grosso state, Brazil. *Precambr. Res.* 111, 91–128.
- Gower, C.F., Ryan, A.B., Rivers, T., 1990. Mid-Proterozoic Laurentia-Baltica: an overview of its geological evolution and a summary of the contributions made by this volume. In: Gower, C.F., Rivers, T., and Ryan, B., (Eds.), *Mid Proterozoic Laurentia-Baltica*. Geological Association of Canada Special Paper, 38, 1–20.

- Guadagnin, F., Chemale Jr., F., 2015. Detrital zircon record of the Paleoproterozoic to Mesoproterozoic cratonic basins in the São Francisco Craton. *J. S. Am. Earth Sci.* 60, 1–13.
- Guadagnin, F., Chemale Jr., F., Magalhães, A.J.C., Santana, A., Dussinim, I., Takehara, L., 2015. Age constraints on crystal-tuff from the Espinhaço Supergroup – Insight into the Paleoproterozoic to Mesoproterozoic intracratonic basin cycles of the Congo-São Francisco Craton. *Gondwana Res.* 27, 363–376.
- Guimaraes, J.T., Teixeira, L.R., Silva, M.G., Martins, A.A.M., Filho, E.L.A., Loureiro, H.S.C., Arcanjo, J.B., Dalton de Souza, J., Neves, J.P., Mascarenhas, J.F., Melo, R.C., Bento, R.V., 2005. Datações U-Pb em rochas magmáticas intrusivas no Complexo Paramirim e no Rife Espinhaço: uma contribuição ao estudo da evolução geocronológica da Chapada Diamantina. III Simpósio sobre o Cráton do São Francisco, Salvador, 159–161.
- Guimaraes, J.T., Martins, A.A.M., Andrade Filho, E.L., Loureiro, H.S.C., Arcanjo, J.B.A., Neves, J.P., Abram, M.B., Silva, M.G., Melo, R.C., Bento, R.V., 2005. Projeto Ibitiara-Rio de Contas Geological map, Brazilian Geological Survey and Bahia Mineral Research Company, scale 1:200,000.
- Halls, H.C., Hamilton, M.A., Denysyn, S.W., 2011. The Melville Bugt dyke swarm of Greenland: A connection to the 1.5–1.6 Ga Fennoscandian Rapakivi Granite Province? In: Srivastava, R.K. (Ed.), *Dyke swarms: Keys for Geodynamic Interpretation*. Springer-Verlag, Berlin, pp. 509–535.
- Hamilton, M.A., Buchan, K.L., 2010. U-Pb geochronology of the Western Channel Diabase, northwestern Laurentia: implications for a large 1.59Ga magmatic province Laurentia's APWP and paleocontinental reconstructions of Laurentia, Baltica and Gawler craton of southern Australia. *Precambr. Res.* 183, 463–473.
- Heaman, L., 1991. U-Pb dating of giant radiating dyke swarms: potential for global correlation of mafic magmatic events. In: Extended Abstracts, International Symposium on Mafic Dykes, São Paulo, Brazil, 7–9.
- Heaman, L.M., Gower, C.F., Perreault, S., 2004. The timing of Proterozoic magmatism in the Pinware terrane of southeast Labrador, easternmost Quebec and northwest Newfoundland. *Can. J. Earth Sci.* 41, 127–150.
- Hoffman, P.F., 1997. Tectonic genealogy of North America. In: Van der Pluijm, B.A., Marshak, S. (Eds.), *Earth Structure: An Introduction to Structural Geology and Tectonics*. McGraw-Hill, New York, pp. 459–464.
- Hoffman, P.F., Halverson, G.P., 2008. The Otavi Group of the Northern Platform and the Northern Margin Zone. In: Miller, R. McG (Ed.), *The Geology of Namibia*, Vol. 2. Geological Survey of Namibia, Windhoek, pp. 13.69–13.136.
- Irving, E., Donaldson, J.A., Park, J.K., 1972. Palaeomagnetism of the Western Channel diabase and associated rocks, Northwest Territories. *Can. J. Earth Sci.* 9, 960–971.
- Irving, E., Baker, J.M., Hamilton, M., Wynne, P.J., 2004. Early Proterozoic geomagnetic field in western Laurentia: implications for paleolatitudes, local rotations and stratigraphy. *Precambr. Res.* 129, 251–270.
- Janasi, V.A., Freitas, V.A., Heaman, L.H., 2011. The onset of flood basalt volcanism, Northern Paraná Basin, Brazil: a precise U-Pb baddeleyite/zircon age for a Chapecó-type dacite. *Earth Planet. Sci. Lett.* 302, 147–153.
- Johansson, Å., 2009. Balticia, Amazonia and the SAMBA connection – 1000 million years of neighbourhood during the Proterozoic? *Precambrian Res.* 175, 221–234.
- Key, R.M., Liyungu, A.K., Njam, F.M., Somwe, V., Banda, J., Mosley, P.N., Armstrong, R.A., 2001. The western arm of the Lufilian Arc in NW Zambia and its potential for copper mineralization. *J. Afr. Earth Sc.* 33, 503–528.
- Kirschvink, J.L., 1980. The least-squares line and plane and the analysis of paleomagnetic data. *Geophys. J. Roy. Astron. Soc.* 62, 699–718.
- Kirschvink, J.L., Kopp, R.E., Raub, T.D., Baumgartner, C.T., Holt, J.W., 2008. Rapid, precise, and high-sensitivity acquisition of paleomagnetic and rock-magnetic data: Development of a low-noise automatic sample changing system for superconducting rock magnetometers. *Geochem. Geophys. Geosyst.* <http://dx.doi.org/10.1029/2007GC001856>.
- Kröner, A., Cordani, U., 2003. African and South American cratons were not part of the Rodinia supercontinent: Evidence from field relationships and geochronology. *Tectonophysics* 375, 325–352.
- Lubnina, N.V., Mertanen, S., Söderlund, U., Bogdanova, S., Vasilieva, T.T., Frank-Kamenetsky, D., 2010. A new key pole for the east European craton at 1452 Ma: Paleomagnetic and geochronological constraints from mafic rocks in Lake Ladoga region (Russian Karelia). *Precambr. Res.* 183, 442–462.
- Maier, W.D., Peltonen, P., Livesey, T., 2007. The ages of the Kabanga North and Kapalagulu intrusions, Western Tanzania: a reconnaissance study. *Econ. Geol.* 102, 147–154.
- Maier, W.D., Rasmussen, B., Fletcher, I.R., Li, C., Barnes, S.-J., Huhma, H., 2013. The Kunene Anorthosite Complex, Namibia, and its satellite intrusions: Geochemistry, geochronology, and economic potential. *Econ. Geol.* 108, 953–986.
- Mäkitie, H., Data, G., Isabyre, E., Manttari, I., Huhma, H., Klausen, M.B., Pakkanen, L., Virransalo, P., 2014. Petrology, geochronology and emplacement model of the giant 1.37 Ga arcuate Lake Victoria Dyke Swarm on the margin of a large igneous province in eastern Africa. *J. Afr. Earth Sc.* 97, 273–297.
- Mayer, A., Hofmann, A.W., Sinigoi, S., Morais, E., 2004. Mesoproterozoic Sm-Nd and U-Pb ages for the Kunene Anorthosite Complex of SW Angola. *Precambr. Res.* 133, 187–206.
- McElhinny, M.W., Powell, C.McA., Pisarevsky, S.A., 2003. Paleozoic terranes of eastern Australia and the drift history of Gondwana. *Tectonophysics* 362, 41–65.
- Meert, J.G., 2002. Paleomagnetic Evidence for a Paleo-Mesoproterozoic Supercontinent Columbia. *Gondwana Res.* 5, 207–215.
- Meert, J.G., Stuckey, W., 2002. Revisiting the palaeomagnetism of the 1.476 Ga St. Francois Mountains igneous province, Missouri. *Tectonics* 21, 1–19.
- Meert, J.G., Hargraves, R.B., Van der Voo, R., Hall, C.M., Halliday, A.N., 1994. Paleomagnetic and  $^{40}\text{Ar}/^{39}\text{Ar}$  studies of Late Kibaran intrusives in Burundi, East Africa: implications for Late Proterozoic supercontinents. *J. Geology* 102, 621–637.
- Meert, J.G., Van der Voo, R., Patel, J., 1994. Paleomagnetism of the Late Archean Nyanzian System, western Kenya. *Precambr. Res.* 69, 113–131.
- Meert, J.G., Van der Voo, R., Ayub, S., 1995. Paleomagnetic investigation of the Late Proterozoic Gagwe lavas and Mbozi complex, Tanzania and the assembly of Gondwana. *Precambr. Res.* 74, 225–244.
- Mertanen, S., Pesonen, 1995. Palaeomagnetic and rock magnetic investigations of the Sipoö Subjotnian quartz porphyry and diabase dykes, southern Fennoscandia. *Phys. Earth Planet. Inter.* 88, 145–175.
- Mitchell, R.N., Evans, D.A.D., Kilian, T.M., 2010. Rapid Early Cambrian rotation of Gondwana. *Geology* 38, 755–758.
- Moakhar, M.O., Elming, S.-Å., 2000. A palaeomagnetic analysis of Rapakivi intrusions and related dykes in the Fennoscandian shield. *Phys. Chem. Earth (A)* 25 (5), 489–494.
- Moloto-A-Kengumba, G.R., Trindade, R.I.F., Monie, P., Nedelec, A., Siqueira, R., 2008. A late Neoproterozoic paleomagnetic pole for the Congo craton: Tectonic setting, paleomagnetism and geochronology of the Nola dike swarm (Central African Republic). *Precambr. Res.* 164, 214–226.
- Neuvonen, K.J., 1986. On the direction of remanent magnetization of the quartz porphyry dikes in SE Finland. *Bull. Geol. Soc. Finland* 58, 195–201.
- Oliveira, E.P., Tarney, J., 1995. Petrogenesis of the Late Proterozoic Curaçá mafic dyke swarm, Brazil: asthenospheric magmatism associated with continental collision. *Mineral. Petrol.* 53, 27–48.
- Oliveira, E.P., McNaughton, N.J., Armstrong, R., 2010. Mesoarchaean to Palaeoproterozoic growth of the northern segment of the Itabuna Salvador Curaçá orogen, São Francisco craton, Brazil. *Geological Society, London, Special Publications*, 338, 263–286.
- Oliveira, E.P., Silveira, E.M., Söderlund, U., Ernst, E.E., 2013. U-Pb ages and geochemistry of mafic dyke swarms from the Uauá Block, São Francisco Craton, Brazil: LIPs remnants relevant for Late Archaean break-up of a supercraton. *Lithos* 174, 308–322.
- Palmer, H.C., Merz, B.A., Hayatsu, A., 1977. The Sudbury dikes of the Grenville Front region: paleomagnetism, petrochemistry, and K-Ar age studies. *Can. J. Earth Sci.* 14, 1867–1887.
- Pavlov, V., Bachtadse, V., Mikhailov, V., 2008. New Middle Cambrian and Middle Ordovician palaeomagnetic data from Siberia: Llandelian magnetostratigraphy and relative rotation between the Aldan and Anabar-Angara blocks. *Earth Planet. Sci. Lett.* 276, 229–242.
- Pavlov, V., Veselovskiy, R., Evans, D.A.D., 2014. Long-lived, tight fit of Siberia and Laurentia in Proterozoic time. GAC® – MAC/AGC – AMC Fredericton 2014 Joint Annual Meeting, Congrès Annuel Conjoint, Abstracts – Résumés Volume 37, 215–216.
- Pedreira, A.J.C.L., 1994. O Supergrupo Espinhaço na Chapada Diamantina Centro-Oriental, Bahia: Sedimentação, Estratigrafia e Tectônica. (Ph.D thesis) Universidade São Paulo.
- Pedreira, A.J., De Waele, B., 2008. Contemporaneous evolution of the Palaeoproterozoic-Mesoproterozoic sedimentary basins of the São Francisco-Congo Craton. In: Pankhurst, R.J., Trouw, R.A.J., Brito Neves, B.B., De Wit, M.J. (Eds.), West Gondwana: Pre-Cenozoic Correlations across the South Atlantic Region. *Geological Society Special Publications*, 294, 33–48.
- Pehrsson, S.J., Eglington, B.M., Evans, D.A.D., Huston, D., Reddy, S.M., 2016. Metallogeny and its link to orogenic style during the Nuna supercontinent cycle. In: Li, Z.X., Evans, D.A.D. and Murphy, J.B. (Eds.), *Supercontinent Cycles Through Earth History*. Geological Society of London Special Publications, 424.
- Persson, A.I., 1999. Absolute (U-Pb) and relative age determinations of intrusive rocks in the Ragunda rapakivi complex, central Sweden. *Precambr. Res.* 95, 109–127.
- Pesonen, L.J., Elming, S.-Å., Mertanen, S., Pisarevsky, S., D'Agrella-Filho, M.S., Meert, J.G., Schmidt, P.W., Abrahamsen, N., Bylund, G., 2003. Palaeomagnetic configuration of continents during the Proterozoic. *Tectonophysics* 375, 289–324.
- Petrovský, E., Kapička, A., 2006. On determination of the Curie point from thermomagnetic curves. *J. Geophys. Res.* 111, B12S27. <http://dx.doi.org/10.1029/2006JB004507>.
- Piper, J.D.A., 1974. Magnetic properties of the Cunene Anorthosite Complex, Angola. *Phys. Earth Planet. Inter.* 9, 353–363.
- Piper, J.D.A., 1979. Palaeomagnetism of the Ragunda intrusion and dolerite dykes, central Sweden. *Geologiska Foreningens I Stockholm Forhandlingar* 101, 139–148.
- Pisarevsky, S., Bylund, G., 2010. Palaeomagnetism of 1780–1770 Ma mafic and composite intrusions of Småland (Sweden): implications for the Mesoproterozoic supercontinent. *Am. J. Sci.* 310, 1168–1186.
- Pisarevsky, S.A., Natapov, L.M., 2003. Siberia and Rodinia. *Tectonophysics* 375, 221–245.
- Pisarevsky, S.A., Natapov, L.M., Donskaya, T.V., Gladkochub, D.P., Vernikovsky, V.A., 2008. Proterozoic Siberia: a promontory of Rodinia. *Precambr. Res.* 160, 66–76.
- Pisarevsky, S.A., Biswal, T.K., Wang, X.-C., De Waele, B., Ernst, R., Söderlund, U., Tait, J.A., Ratre, K., Singh, Y.K., Cleve, M., 2013. Palaeomagnetic, geochronological and geochemical study of Mesoproterozoic Lakhna Dykes in the Bastar Craton, India: implications for the Mesoproterozoic supercontinent. *Lithos* 174, 125–143.

- Pisarevsky, S.A., Elming, S., Pesonen, L.J., Li, Z.-X., 2014. Mesoproterozoic paleogeography: Supercontinent and beyond. *Precambr. Res.* 244, 207–225.
- Poidevin, J.-L., 2007. Stratigraphie isotopique du strontium et datation des formations carbonatées et glaciogéniques néoprotérozoïques du Nord et de l'Ouest du craton du Congo. *C.R. Geosci.* 339, 259–273.
- Puchkov, V.N., Bogdanova, S.V., Ernst, R.E., Kozlov, V.I., Krasnobaev, A.A., Wingate, M.T.D., Postnikov, A., Sergeeva, N.D., 2013. The ca. 1380 Ma Mashak igneous event of the Southern Urals. *Lithos* 174, 109–124.
- Rainbird, R.H., Stern, R.A., Khudoley, A.K., Kropachev, A.P., Heaman, L.M., Sukhorukov, V.I., 1998. U-Pb geochronology of Riphean sandstone and gabbro from southeast Siberia and its bearing on the Laurentia-Siberia connection. *Earth Planet. Sci. Lett.* 164, 409–420.
- Rapalini, A.E., Sánchez Bettucci, L., Badgen, E., Vásquez, C.A., 2015. Paleomagnetic study on mid-Paleoproterozoic rocks from the Rio de la Plata craton: implications for Atlantica. *Gondwana Res.* 27, 1534–1549.
- Reis, N.J., Teixeira, W., Hamilton, M.A., Bispo-Santos, F., Almeida, M.E., D'Agrella-Filho, M.S., 2013. Avanavero mafic magmatism, a late Paleoproterozoic LIP in the Guiana Shield, Amazonian Craton: U-Pb ID-TIMS baddeleyite, geochemical and paleomagnetic evidence. *Lithos* 174, 175–195.
- Renne, P.R., Onstott, T.C., D'Agrella-Filho, M.S., Pacca, I.G., Teixeira, W., 1990. 40Ar/39Ar dating of 1.0–1.1 Ga magnetizations from the São Francisco and Kalahari cratons: tectonic implications for Pan-African and Brasiliano mobile belts. *Earth Planet. Sci. Lett.* 101, 349–366.
- Rogers, J.J.W., Santosh, M., 2002. Configuration of Columbia, a Mesoproterozoic supercontinent. *Gondwana Res.* 5, 5–22.
- Salminen, J., Pesonen, L.J., 2007. Paleomagnetic and rock magnetic study of the Mesoproterozoic sill, Valaam island, Russian Karelia. *Precambr. Res.* 159, 212–230.
- Salminen, J.M., Klein, R., Veikkolainen, T., Mertanen, S., Mänttäri, I., submitted. Mesoproterozoic geomagnetic reversal asymmetry in light of new paleomagnetic and geochronological data for the Häme dyke swarm, Finland: Implications for the Nuna supercontinent. *Precambr. Res.*
- Salminen, J., Mertanen, S., Evans, D.A.D., Wang, Z., 2014. Paleomagnetic and geochemical studies of the Mesoproterozoic Satakunta dyke swarms, Finland, with implications for a Northern Europe – North America (NENA) connection within Nuna supercontinent. *Precambr. Res.* 244, 170–191.
- Salminen, J.M., Klein, R., Mertanen, S., Pesonen, L.J., Fröjdö, S., Mänttäri, I., Eklund, O., 2016. Palaeomagnetism and U-Pb geochronology of ca. 1570 Ma intrusives from Åland archipelago, SW Finland – implications for Nuna. In: Li, Z.X., Evans, D.A.D. and Murphy, J.B. (Eds.), *Supercontinent Cycles Through Earth History*. Geological Society of London Special Publications, 424. doi:10.1144/SP424.3.
- Shcherbakova, V.V., Lubnina, N.V., Shcherbakov, V.P., Mertanen, S., Zhidkov, G.V., Vasiliieva, T.I., Tsel'movich, V.A., 2008. Palaeointensity and palaeodirectional studies of early Riphean dyke complexes in the Lake Ladoga region (Northwestern Russia). *Geophys. J. Int.* 175, 433–448.
- Silveira, E.M., Söderlund, U., Oliveira, E.P., Ernst, R.E., Menez Leal, A.B., 2013. First precise U-Pb baddeleyite ages of 1500 Ma mafic dykes from the São Francisco Craton, Brazil, and tectonic implications. *Lithos* 174, 144–156.
- Tack, L., Wingate, M.T.D., Liégeois, J.-P., Fernandez-Alonso, M., Deblond, A., 2001. Early Neoproterozoic magmatism (1000–910 Ma) of the Zadinian and Mayumbian Groups (Bas-Congo): onset of Rodinia rifting at the western edge of the Congo craton. *Precambr. Res.* 110, 277–306.
- Tack, L., De Wingate, M.T.D., Waele, B., Meert, J., Belousova, E., Griffin, B., Tahon, A., Fernandez-Alonso, M., 2010. The 1375 Ma "Kibaran event" in Central Africa: prominent emplacement of bimodal magmatism under extensional regime. *Precambr. Res.* 180, 63–84.
- Teixeira, W., Figueiredo, M.C.H., 1991. An outline of Early Proterozoic crustal evolution in the São Francisco craton, Brazil: a review. *Precambr. Res.* 53, 1–22.
- Teixeira, W., Sabaté, P., Barbosa, J., Noce, C.M., Carneiro, M.A., 2000. Archean and Paleoproterozoic tectonic evolution of the São Francisco Craton. In: Cordani, U.G., Milani, E.J., Thomaz Filho, A., Campos, D.A. (Eds.), *Tectonic Evolution of South America: 31st International Geological Congress, Rio de Janeiro*, pp. 107–137.
- Trindade, R.I.F., D'Agrella-Filho, M.S., Babinsky, M., Font, E., Brito Neves, B.B., 2004. Paleomagnetism and geochronology of the Bebedouro cap carbonate: evidence for continental-scale Cambrian remagnetization in the São Francisco craton, Brazil. *Precambr. Res.* 128, 83–103.
- Trompette, R., 1994. *Geology of Western Gondwana (2000–500 Ma)*. A.A. Balkema, Rotterdam/Brookfield, p. 350.
- Van der Voo, R., 1990. The reliability of paleomagnetic data. *Tectonophysics* 184, 1–9.
- Verwey, E.J.W., 1939. *Nature* 144, 327.
- Williams, H., Hoffman, P.F., Lewry, J.F., Monger, J.W.H., Rivers, T., 1991. Anatomy of North America: Thematic geologic portrayals of the continent. *Tectonophysics* 187, 117–134.
- Wingate, M.T.D., Pisarevsky, S.A., Gladkochub, D.P., Donskaya, T.V., Konstantinov, K.M., Mazukabzov, A.M., Stanevich, A.M., 2009. Geochronology and paleomagnetism of mafic igneous rocks in the Olenek Uplift, northern Siberia: implications for Mesoproterozoic supercontinents and paleogeography. *Precambr. Res.* 170, 256–266.
- Wu, H., Zhang, S., Li, Z.X., Li, H., Dong, J., 2005. New paleomagnetic results from the Yangzhuang Formation of the Jixian System, North China, and tectonic implications. *Chin. Sci. Bull.* 50, 1483–1489.
- Xu, H., Yang, Z., Peng, P., Meert, J.G., Zhua, R., 2014. Paleo-position of the North China craton within the supercontinent Columbia: Constraints from new paleomagnetic results. *Precambrian Res.* 255, 276–293.
- Zhang, S., Li, Z.-X., Evans, D.A.D., Wu, H., Li, H., Dong, J., 2012. Pre-Rodinia supercontinent Nuna shaping up: a global synthesis with new paleomagnetic results from North China. *Earth Planet. Sci. Lett.* 353–354, 145–155.
- Zhao, G., Sun, M., Wilde, S.A., Li, S., 2004. A Paleo-Mesoproterozoic supercontinent: assembly, growth and breakup. *Earth Sci. Rev.* 67, 91–123.